ANALYSIS

OF

THE RATES OF CONSOLIDATION

FOR

PEAT

ANALYSIS

OF

THE RATES OF CONSOLIDATION

FOR

PEAT

by

MEI-MAN LO, B.S.

A Thesis

Submitted to the Faculty of Graduate Studies

in Partial Fulfilment of the Requirements

for the Degree

Master of Engineering

McMaster University

May 1964

MASTER OF ENGINEERING (1964) McMASTER UNIVERSITY
(Civil Engineering) Hamilton, Ontario.

TITLE: Analysis of the Rates of Consolidation for Peat

AUTHOR: Mei-ban Lo, B.Sc. (National Taiwan University)

SUPERVISOR: Professor N. E. Wilson

NUMBER OF PAGES: v, 64

SCOPE AND CONTENTS:

An analysis of peat consolidation on the basis of consolidation rates is described. The effects of sample height, applied stress and initial void-ratio on consolidation were studied. Equations describing the rates of consolidation in the laboratory were derived and transferred to nomographic form.

ACKNOWLEDGEMENTS

The author wishes to thank Professor N. E. Wilson for the help and encouragement received during the course of this research.

Thanks are also due to Mr. M. R. Krzywicki for the help in preparing this thesis.

Finally, the author wishes to acknowledge the financial assistance made available to this project from the Defence Research Board of Canada (Grant Number 9768-04).

TABLE OF CONTENTS

TABLE OF CONTENTS (Continued)

INTRODUCTION

According to estimates, 500,000 square miles of Canada are covered by peat or muskeg as it is traditionally called. This amounts to approximately 12 per cent of the area of this country. Most of this organic terrain, which varies from a few inches to a couple of hundred feet in thickness, occurs in the northern part of Canada, but a substantial amount also occurs in the more southerly regions of the country, as well as in the northern United States.

These muskeg areas are generally so soft that they present a serious access problem, whether by ordinary off-road vehicles or in the construction of highways. Therefore, several major engineering problems must be solved before this area can be developed. The first soil engineering problem encountered in developing an area is to determine the characteristics of consolidation of the soil. Upon these characteristics of consolidation, the prediction and control of settlements of roads and buildings depend.

The classical methods of analysis based upon the mathematical approach developed by Terzaghi (Terzaghi, 1925) do not appear entirely applicable to the consolidation of peat, possibly due to the complexity of the structure and the composition. It is possible that another mathematical approach may more adequately describe the consolidation of peat. This thesis presents a new analysis in graphical form for the prediction of settlements. This graphical representation makes it possible to construct a nomograph which predicts the behaviour under load of the peat tested.

CHAPTER 1

Literature Review

Consolidation of Soils

When a load is applied to the soil, the water pressure in the pores is generated. This is known as pore-water pressure. The pore-water pressure will dissipate slowly because of the low permeability of the soil. The process of the dissipation of the pore-water pressure and the subsequent compression of the soil mass is called consolidation.

Terzaghi introduced a model to demonstrate the process of consolidation in his classic paper (Terzaghi, 1925). The model consisted of a cylindrical vessel, containing a perforated piston supported by springs. The vessel was filled with water to the top of the piston. When a load was applied to the piston, the load was carried entirely by the water under excess hydrostatic pressure. After a short time, some water escaped through the piston, and the height of the spring decreased. The load, carried by the water under pressure, transferred to the spring until the load was carried entirely by the spring. The decrease in the height of the spring is considered to be equivalent to the settlement of soil during consolidation.

Using this model, Terzaghi developed the theory of one-dimensional consolidation. Terzaghi's theory implies that for any load a final void-ratio is reached. This theory does not explain the phenomenon of secular

time effect (secondary consolidation) obtained in long term consolidation tests in the laboratory. Buisman derived a formula for this secular time effect based on field settlement observations of embankments and structures and on test results of undisturbed soil samples (Buisman, 1936). Koppejan derived another formula combining the Terzaghi load-compression relationship and the Buisman secular time effect (Koppejan, 1948). The validity of this formula was lessened by forcing the data to fit the formula.

Taylor investigated the disagreement between the Terzaghi consolidation theory and the behaviour during laboratory consolidation tests (Taylor, 1942). In this paper, Theory A and Theory B were established. Theory A, which is based upon Terzaghi's equation for one-dimensional consolidation, assumed that the speed of occurrence of secondary compression is proportional to the undeveloped secondary compression. The value from Theory A approaches the value given by Terzaghi's theory for thicker layers. Theory B, which has a distinguishing characteristic, is based on the assumption that plastic resistance to compression exists in clay. The magnitude of plastic resistance is dependent on the speed of compression. The plastic resistance at the termination of primary compression has been defined as "Bond" of clay.

Suklje developed an isotaches method for the analysis of the consolidation process (Suklje, 1957). In this method, the compressibility of a soil was described by a system of isotaches (effective vertical stress versus average void ratio). The isotaches were obtained from consolidation curves of consolidometer tests carried out for various load

increments. The variability of the coefficient of permeability with the process of consolidation was taken into account. This was assumed constant in Terzaghi's and Taylor's theories.

Tan interpreted the secular time effect by applying rheological models (Tan, 1954). Three-dimensional differential equations were derived for the consolidation of clay. Solutions were obtained for certain boundary conditions.

The behaviour of soil consolidation under different ratios of load increment has been studied (Newland and Allely, 1960; Leonards and Girault, 1961). The results of their investigations provided the clue to secondary compression characteristics of soils.

Consolidation with Special Respect to Peat

Hanrahan studied the engineering properties of peat in Ireland and showed both the discrepancy between the properties of peat and clay and also the great variability of peat, even within the samples from one bog (Hanrahan, 1954). He showed that the standard methods of curve-fitting, i.e., Casagrande (1936), Taylor (1942), Naylor and Doran (1948), used in connection with clays have little application in forecasting settlements in peat. Limited agreement was achieved by the method of Koppejan (1948).

In Japan, research into the engineering characteristics of peat has been conducted at the Hokkaido Development Bureau under the direction of Miyakawa. Miyakawa derived a coefficient of secondary compression $C_s = b/H$, where b is the rate of settlement of the secondary phase for one cycle on the log t scale and H is the thickness of the compressible

layer. C_s increases with the consolidation pressure up to the pre-consolidation pressure. It was proved that the preload method is effective for decreasing the effect of secondary consolidation.

From studies of peat in Scotland, Lake showed that the presence of sand drains increased the rate of dissipation of excess pore water pressure in the peat, but was not accompanied by a significant change in the speed of consolidation as observed in clay consolidation (Lake, 1960).

Brawner showed that the rate of secondary compression, after the pore water pressure has dissipated, is independent of the drainage conditions and is thus theoretically independent of the thickness of the peat layer (Brawner, 1961).

Enright and Adams suggested that the "initial" consolidation (or primary consolidation) of peat is due to the rapid expulsion of free water in the peat mass, while the "longer term" consolidation (or secondary consolidation) is due to the slow expulsion of the held water in the "solid" material (Enright and Adams, 1963). The primary consolidation and secondary consolidation were separated arbitrarily at the point where the linear relationship starts in the settlement-time curve. Initial settlement and rate of secondary consolidation were plotted separately for various peat thicknesses and various applied loads. Total settlement at any time is the sum of the initial settlement and the secondary settlement.

Schroeder and Wilson studied the rheological characteristics at McMaster University and showed that the rate of drainage governs the

primary part of peat consolidation, whereas the plastic or viscous characteristic governs the secondary part. Drainage flow and viscous flow were separated and plotted on a rheological diagram ($\frac{d\varepsilon}{dt} - \bar{\sigma}$; axial strain rate versus axial effective stress). (Schroeder and Wilson, 1962).

It is believed that the rate of compression is the key to the consolidation of peat. Using this assumption, the peat consolidation is studied and described in this thesis.

CHAPTER 2

Physical Properties of Amorphous-granular Peat

The material used in this research project was amorphous-granular peat. The peat was obtained two feet below the surface of a lake near Parry Sound, Ontario. This material is dark grey in colour and is composed of fine organic fibers and mineral particles. The vegetal cover is classified as FI, according to the Radforth classification system (Radforth, 1952). The soil is within the peat range on the plasticity chart (Casagrande, 1948; Fig. 1).

The sample, which was obtained from the field, had the consistency of a thick slurry. The water content, after removal from the lake bottom, was in the region of 600 to 700% of the dry weight. The specific gravity of the sample was within the range of 1.95 to 2.05. The liquid limit was 390% and the plastic limit 170%. The ignition loss was 25.5% of oven dried weight.

A grain size analysis was attempted on this material by washing a portion through a series of standard sieves (U. S. Bureau of Standards), ranging in size from the #10 to #200 and then conducting a hydrometer analysis. The results of these analyses are shown in Fig. 2. The grain size analysis of peat using methods presently employed in the field of soil mechanics is not valid. This is substantiated by the fact that the fibrous material in the peat wrapped around the wire in the screen. The hydrometer analysis is based on the validity of Stokes' law. The basic assumption in this law is that the material is composed of individual

spherical grains without any tendency to flocculate. As peat is a fibrous material, this basic assumption cannot be made.

It was found by performing a series of viscosity measurements with a Brookfield rotational viscometer that the material behaves as a thixotropic pseudo-plastic. A rheological diagram is shown in Fig. 3. Additional information regarding rheological properties of peat has been presented by Schroeder and Wilson (Schroeder and Wilson, 1962).

CHAPTER 3

Apparatus, Preparation of Samples and Test Procedures

Apparatus

Two large consolidometers were designed to consolidate the sample from a slurry. A consolidometer (Fig. 4) is composed of two aluminum cylinders, 6 1/8 inches inside diameter. The upper cylinder is 10 inches high and the lower cylinder is 4 1/2 inches. A piston (2 1/8 inches thick, 6 inches diameter) was connected to a loading platform by means of a hollow aluminum shaft (1 inch outside diameter). The piston was fitted with two O-rings to prevent leakage past the piston. The bottom of the piston was fitted with a porous stone (Norton, P? 120, 1/2 inch thick, 6 1/16 inches in diameter) which allowed the passage of pore water. A similar porous stone was placed at the bottom of the cylinder to allow the measurement of pore water pressures at the base of the sample. A valve was located at the bottom of the cylinder beneath the bottom porous stone. An overflow hole was drilled at the top of the consolidometer to maintain a constant water level in the consolidometer throughout the test.

A section of plastic tube (2 mm I.D., 2 feet long) was connected from the valve to an open mercury manometer which consisted of a U-shaped capillary tube (1 mm I.D.) with mercury reservoir in one leg. A valve on top of this leg was used to remove the air from the system. The manometer was so arranged to compensate for capillary effect, that the excess hydrostatic pressure reading was zero when the consolidometer was filled with water.

A dial gauge was used to record the settlement of the loading platform during the test.

The piston, including the loading platform and shaft weighed 18 pounds. This reduced to 15 pounds after the piston was submerged in the water.

Preparation of Samples and the Test Procedures

Before assembly of the apparatus, the porous stones used were soaked in distilled water for one hour to reduce the air content in them. The plastic tube connected to the manometer was filled with water from the top of valve A (Fig. 4) and then the valve was closed.

The sample, after its removal from the field, was covered with free water and stored in a humid room (R.H. 85 to 95% at 23°C). During sample preparation, the free water covering the sample was drained. The sample was then mixed to obtain uniformity throughout the sample.

The sample was then poured slowly into the consolidometer to minimize turbulence and trapping of air. The top of the sample was leveled with a spatula. The height of the sample was recorded to serve as an approximate check on the height calculated from the data at the end of the test.

The other end of the plastic tube was then connected to the valve at the bottom of the consolidometer. The valve was opened. The piston was then lowered slowly into the consolidometer until contact was made with the sample. The point of contact was indicated by the movement of the mercury column in the manometer, which indicated pore water pressure. When contact was made, a support was placed between the [illegible] of the con-

solidometer and the loading platform to keep the piston load off the sample. The consolidometer was filled with water to the overflow level. A predetermined load was then placed on the loading platform. The dial gauge was placed in contact with the platform and set to zero.

The test was started at a convenient time by removing the support which kept the applied load off the sample. Settlements in thousandths of an inch and pore water pressure in millimeters of mercury column were recorded at various time intervals.

A settlement versus logarithm of time curve (S - log t; Fig. 5) was plotted as the test progressed. A test was stopped after the S - log t curve had changed from a downward concave curve to an upward concave curve.

In dismantling the apparatus, the water in the cylinder was drained by a siphon. The load was taken off and the piston was removed. The sample was removed from the consolidometer as quickly as possible and the final height of the sample was measured to the nearest quarter of a millimeter. One section of the sample was weighed and dried at 95°C for 24 hours for the determination of the final water content. The temperature of 95°C was chosen to minimize the loss of the organic material in the drying process.

The initial height of the sample was calculated from the final height of the sample and the total settlement measured, assuming that the rebound of the sample in disassembling was negligible.

$$H_i = H_f + S_{total}$$

The average void-ratios during the process of consolidation were calculated from the water content and the specific gravity

$$e = w \times G$$

This is based on the assumptions that the void-ratio is proportional to the height of the sample and the sample was fully saturated before the test began.

The net applied load was determined by subtracting the load required to overcome the friction between the O-rings and the cylinder wall from the total applied load.

The friction was found to be a function of piston speed and certain conditions of lubrication. The procedure which was used to determine the frictional components is described in the Appendix.

All the measurements which were taken using the metric system were converted to the British system.

Many parameters, such as sample height, applied stress, initial void-ratio, atmospheric pressure and temperature changes, etc., influence the consolidation characteristics. The influences of each of these were studied in the laboratory. Tests were conducted with variations of one of these parameters, as the others were kept constant. These tests were conducted with variation of sample height, applied stress and initial void-ratio and readings were made of the atmospheric pressure and temperature changes.

CHAPTER 4

Analysis of Consolidation of Rates

Analysis Method

A consolidation analysis using the rates of consolidation is described in this chapter. The rate of consolidation, $\frac{de}{dt}$, is defined as the change of average void-ratio in an infinitesimal time interval and has the unit min^{-1}.

After each test, the average void-ratios during the test were calculated from the final water content and the settlements; fig. 6 shows the average void-ratios plotted versus elapsed time. The rates of consolidation were calculated from any two successive void-ratio values. Fig. 7, where the rates of consolidation versus times were plotted on a log-log paper, shows that two tangents to a short curve exist. When the two straight line portions of the curve were extended to their point of intersection, the straight line portion with a smaller value of elapsed time is called the "Early-Stage" of consolidation. The slope of the straight line portion is flatter in "Early-Stage" of consolidation than in "Late-Stage" of consolidation.

For each stage of the consolidation, the following relationship could be conjectured,

$$\log \frac{de}{dt} = k \log t + \log C, \qquad (1)$$

where k is the slope of the straight line and is negative.

By definition, C is the value of $\frac{de}{dt}$ at t = 1 minute, and is called "Initial Rate". The C value of the "Late-Stage" consolidation is obtained by extending the straight line portion of "Late-Stage" to t = 1 minute. The subscripts 1 and 2 for K and C are used to denote the "Early-Stage" and "Late-Stage" consolidation respectively.

Formula (1) can be written as

$$\log \left(\frac{de}{dt}/t^{k}\right) = \log C$$

or

$$\frac{de}{dt} = C \cdot t^{k}$$

It can be seen that the rates of consolidation are a function of time and are equal to $C_1 t^{k_1}$ in "Early-Stage", $C_2 t^{k_2}$ in "Late-Stage" of consolidation.

The "Early-Stage" and "Late-Stage" of consolidation are analogous to "Primary" and "Secondary" consolidation. The time when the consolidation changes from "Early-Stage" to "Late-Stage" is called the "End of Early-Stage" of consolidation and is denoted by t_t. This was compared with the time of 100% primary consolidation obtained by the logarithm time fitting method (Chapter 6).

Pore-water Pressure

The typical pore-water pressure dissipation curve is shown in Fig. 5. In the first quarter minute after the sample has been loaded, the pore-water pressure increased rapidly to approximately 95% of the theoretical maximum pore-water pressure and then increased at a slow rate until the maximum value was reached. The pore-water pressure dissipated after the maximum value and dropped to approximately zero after the "End

The maximum pore-water pressures versus applied stresses are shown in Fig. 8; the applied stresses are the net stresses after an allowance for piston friction. The accuracy for pore-water pressure measurements was ± 0.02 lb/in.^{2} and this accuracy is also a function of the time at which the pore-water pressure reaches a maximum and the hydrodynamic lag in the instrument.

It is noted in Fig. 8 that the maximum pore-water pressure for a series of replicate samples loaded under various loadings* are generally equal to the net applied stresses.

*This series of tests is described as P II tests in Chapter 5.

CHAPTER 5

The Influences of Various Parameters on the Rates of Consolidation

Parameters

It was found that the three parameters, the sample height (H_i, or drainage path), the applied stresses (σ) and the initial void-ratio (e_i) are the most important factors affecting the characteristics of peat consolidation. Other factors, such as the change of temperature and atmospheric pressure, affect the settlement of the sample but are small compared with the settlement due to the consolidation in the "Early-Stage". These effects can be neglected. The effects of the change of temperature and atmospheric pressure on the settlement are significant in the "Late-Stage" of consolidation. These effects are shown by the scattered points (Figures 9, 10, and 11). An attempt was made to minimize the effects due to the change of temperature and atmospheric pressure by completing the test within 10 hours during the day.

To evaluate the individual influence of the sample height, applied stress and initial void-ratio, three series of tests were designed and conducted.

Influence of Sample Height (P I Tests)

In the first series, peat with the same initial void-ratio (Ave.e = 13.47) was used to prepare samples of various heights (H_i ranging from 0.27 to 6.45 in.) and was loaded under the same applied stress (σ = 3.63 lb/in^2.). The influence of initial void-ratio and applied stress was minimized in this series. The data are summarized in Table 1.

Influence of Applied Stress (P II Tests)

In the second series, peat with the same initial void-ratio (Ave. e_i = 10.84) was used to prepare the samples of the same height (Ave. H_i = 0.92 in.) and was loaded under various applied stresses (σ ranging from 0.45 to 7.03 lb/in^2). The influence of initial void-ratio and sample height was minimized in this series. The data are summarized in Table 2. (All the analysis data are shown in Table 4.)

Influence of the Initial Void-Ratio (P III Tests)

In the third series, peat with various initial void-ratio (e_i ranging from 8.62 to 12.40) were used to prepare the samples ~~of the samples~~ of the same height (Ave. H_i = 0.96 in.) and was loaded under the same applied stress (σ = 3.63 lb/in^2). The influence of sample height and applied stress was minimized in this series. The data are summarized in Table 3.

The Nomograph

The rates of consolidation versus time for P I, P II and P III tests were plotted on a log-log scale (Fig. 9, 10 and 11). It was found that the slopes of the straight line portion of all these curves are the same for the "Early-Stage (k_1 = -0.6) and similarly for the "Late-Stage" consolidation (k_2 = -2.9). Because of the pattern of these curves, a nomograph with two sets of parallel lines can be constructed (Fig. 12). The slopes of these two sets of parallel lines are equal to -0.6 and -2.9. The rates of consolidation of this particular material can be predicted from this nomograph if the initial rate and the time to the "End of Early-Stage" consolidation are known.

Initial Rate

The initial rates, C_1 and C_2, which are defined as the rates when t = 1 minute for "Early-Stage" and "Late-Stage" consolidation, are plotted versus sample height for the P I tests in Fig. 13A. The C_1 and C_2 values are plotted versus applied stress for the P II tests (Fig. 13B) and versus initial void-ratio for the P III tests (Fig. 13C).

A formula of the initial rate can be derived from these three graphs for the "Early-Stage" and "Late-Stage" consolidation respectively.

$$C_1 = \left(\frac{de}{dt}\right)_{t=1} = \frac{\sigma^{0.34}\, e_i^{2.07}}{10^{(2.63+0.17\, H_i)}}, \quad \text{for "Early-Stage"} \qquad (3)^*$$

$$C_2 = \left(\frac{de}{dt}\right)_{t=1} = \frac{10^{(3.53+H_i)}}{\sigma^{0.23}}, \quad \text{for "Late-Stage"} \qquad (4)$$

where H_i is the sample height in inches, σ is the applied stress in lb/in^2 and e_i is the initial void-ratio.

The Time to the "End of Early-Stage" Consolidation

The time to the "End of Early-Stage" consolidation, t_t, is plotted versus consolidation rates and sample height for the P I tests in Fig. 14. The time, t_t, is plotted versus applied stress for P II tests (Fig. 15) and is plotted versus initial void-ratio for the P III tests (Fig. 16). From these graphs, it was found that the time to the "End of Early-Stage" consolidation is a function of sample height, applied stress and initial void-ratio. The following formula can be derived for Fig. 14, 15 and 16.

$$t_t = \frac{750\, H_i^{1.95}}{\sigma^{0.3}\, e_i^{0.83}} \qquad (5)$$

* See Appendix II.

The effective stresses are changing during the process of consolidation due to the dissipation of pore-water pressures. Due to the complexity of the consolidation characteristics of peat, a simple relationship between the effective stresses and consolidation time does not exist. The time to the "End of Early-Stage" consolidation has been derived as a function of applied stress for the purpose of simplification.

These formulae are based upon the experimental results obtained from laboratory tests and are valid only for this particular type of peat. For any other type, the validity of this approach must be checked.

Estimation of Settlement

From formula (2),

$\frac{de}{dt} = C_1 t^{k_1}$, for "Early-Stage" consolidation, the change of void-ratio in "Early-Stage" consolidation can be obtained by integration.

$$\Delta e_1 = \int_1^{t_t} \frac{de}{dt}\, dt$$

$$= \int_1^{t_t} C_1 t^{k_1}\, dt = \frac{C_1}{k_1+1} \left[t^{k_1+1}\right]_1^{t_t} = \frac{C_1}{k_1+1} \left[t_t^{k_1+1} - 1\right] \qquad (6)$$

if $k_1 \neq -1$.

Similarly, from formula (2),

$\frac{de}{dt} = C_2 t^{k_2}$, for "Late-Stage" consolidation, the change of void-ratio at any time in "Late-Stage" consolidation from the "End of Early-Stage" consolidation is

$$\Delta e_2 = \int_{t_t}^{t_2} \frac{de}{dt}\, dt$$

$$= \int_{t_t}^{t_2} C_2\, t^{k_2}\, dt = \frac{C_2}{k_2+1}\left[t^{k_2+1}\right]_{t_t}^{t_2} = \frac{C_2}{k_2+1}\left[t_2^{k_2+1} - t_t^{k_2+1}\right] \quad (7)$$

where $t_t < t_2 < \infty$; $k_2 \neq -1$

If the straight line portion in the "Late-Stage" consolidation is continuous for an infinite time (Fig. 5), the ultimate settlement can be calculated by setting $t_2 \to \infty$ in formula (7).

$$\Delta e_{\substack{2 \\ t_2 \to \infty}} = \frac{C_2}{k_2+1}\left[t_2^{k_2+1} - t_t^{k_2+1}\right] = \frac{C_2}{k_2+1}\left[\frac{1}{\infty} - t_t^{k_2+1}\right]$$

$$= -\frac{C_2}{k_2+1}\left[t_t^{k_2+1}\right] \quad (8)$$

where $k_2 \neq -1$

The only unknown in this formula is t_t, the time to the "End of Early-Stage" consolidation. The total settlement can be calculated from

$$\Delta e_{total} = \Delta e_1 + \Delta e_2 + \delta e \quad ,$$

where δe is the change of void-ratio in the first one minute and has not been evaluated in this work.

In the above calculations, C values are given in formula (3) and (4), t_t in formula (5) and $k_1 = -0.6$, $k_2 = -2.9$ for this particular peat. Then the assumptions that $k_1 \neq -1$ and $k_2 \neq -1$ are valid for this peat.

Numerical Example

To apply the nomograph, the C_1 and t_t values are evaluated. For $H_i = 1$ in., $\sigma = 4$ lb/in.^{2} and $e_i = 12$, then

$$C_1 = \frac{4^{0.34} \times 12^{2.07}}{10^{(2.63 + 0.17)}} = \frac{1.6 \times 172}{630} = 0.44 \ (\text{min.}^{-1})$$

$$C_2 = \frac{10^{(3.53 + 1)}}{4^{0.23}} = \frac{33900}{1.376} = 2.46 \times 10^4 \ (\text{min.}^{-1})$$

$$t_t = \frac{750 \times 1}{4^{0.3} \times 12^{0.83}} = \frac{750}{1.516 \times 7.80} = 63 \ (\text{min.})$$

The consolidation rates of the sample follow the line with a slope of $k_1 = -0.6$ in the nomograph starting $\frac{de}{dt} = 0.44 \ (\text{min.}^{-1})$, and changes to the line with the slope of $k_2 = -2.9$ after $t_t = 63$ (min.). This example is shown by the dotted line in Fig. 12.

The change of void ratio in the "Early-Stage" consolidation for this sample is

$$\Delta e_1 = \frac{C_1}{k_1+1}\left[t_t^{k_1+1} - 1\right] = \frac{0.44}{0.4}\left[63^{0.4} - 1\right] = \frac{0.44}{0.4}(5.25 - 1) = 4.7$$

while the change of void-ratio in the "Late-Stage" consolidation, for example, from 63 to 100 min. is

$$\Delta e_2 = \frac{C_2}{k_2+1}\left[t_2^{k_2+1} - t_t^{k_2+1}\right] = -\frac{2.46 \times 10^4}{1.9} \times \left[\frac{1}{100^{1.9}} - \frac{1}{63^{1.9}}\right]$$

$$= -\frac{2.46 \times 10^4}{1.9}\left[\frac{1}{6360} - \frac{1}{2600}\right] = \frac{2.46 \times 3.7 \times 10^7}{1.9 \times 1.6 \times 10^7} = 3.0$$

$$\Delta e_{total} = \Delta e_1 + \Delta e_2 + \delta e = 4.7 + 3.0 = 7.7$$

by assuming δe is negligible and

$$\Delta e_{\substack{2 \\ t_2 \to \infty}} = \frac{C_2}{k_2+1}\left[t_t^{k_2+1}\right] = \frac{2.46 \times 10^4}{1.9} \times \frac{1}{2.6 \times 10^3} = 5.0$$

when $t_2 \to \infty$

CHAPTER 6

Comparison of Analysis Methods

The consolidation characteristics obtained by the analysis of rates, can be compared with the characteristics obtained from the Casagrande logarithm time fitting method. The Casagrande method was originally developed for clay.

Separation of Consolidation Process

By Casagrande logarithm time fitting method, the time to the 100% primary consolidation (t_1) is defined as the time to the point where the tangents to the e-log t curve intersect. By the method described in this thesis, the time to the "End of Early-Stage" consolidation (t_t), which is analogous to the time to the 100% primary consolidation, is defined as the elapsed time to the point where the tangents of the two straight line portions of the log $\frac{de}{dt}$ - log t curve intersect.

The time to the 100% primary consolidation (t_1) and the time to the "End of Early-Stage" consolidation (t_t), together with the time to the point where the pore-water pressure has dissipated to almost zero (t_w) are plotted for the P II test (Fig. 17). The time to the 100% primary consolidation is longer than that to the "End of Early-Stage" consolidation.

The time to the "End of Early-Stage" consolidation (P III 2 test) is indicated by point A (Fig. 5). Point A occurs before the s-log t curve becomes concave upward. Previously, if an s-log t (or e-log t)

curve did not exhibit an upward concave curve, the point of 100% primary consolidation could not be determined (Lo, 1961; Wahls, 1962). As point A occurs before the upward concave curve, it is possible by the method proposed to separate the consolidation process into two parts, i.e., "Early-Stage" and "Late-Stage" consolidation.

Void-Ratio at the "End of Early-Stage" Consolidation

The void-ratio at 100% primary consolidation as obtained by Casagrande logarithm time fitting method and the void-ratio at the "End of Early-Stage" consolidation both are plotted versus applied stress for P II tests (Fig. 18). If the void-ratio at 100% primary consolidation and the void-ratio at the "End of Early-Stage" consolidation both are plotted versus sample height or initial void-ratio, similar parallel relationships exist.

CHAPTER 7

Conclusions

Terzaghi developed the theory of one-dimensional consolidation in 1925 (Terzaghi, 1925). His theory, however, does not explain the phenomenum of "secular" effect obtained in long term consolidation tests in the laboratory. In the literature, the designation "primary" consolidation has been applied to the excess pore water pressure phase of the consolidation process and "secondary" consolidation to that phase of the consolidation beyond the pore-water pressure phase. These two phases of consolidation are arbitrarily divided by graphical methods based on the dissipation of pore-water pressure, measured during the consolidation tests.

The literature has shown that this classical approach to consolidation is not entirely applicable to peats and many difficulties have arisen. A more rigid and meaningful definition of the "primary" and "secondary" phases of consolidation as well as the methods used in dividing them are indicated.

In this investigation an analysis of peat consolidation in the laboratory has been developed, based on rates of consolidation. The relationship conjectured on the log $\frac{de}{dt}$ - log t plot was established and it was found that the consolidation process can be divided into "Early-Stage" and "Late-Stage" consolidation, characterised by the change in slopes of the fitted line on a log $\frac{de}{dt}$ - log t plot. The "Early-Stage" and "Late-Stage" consolidation can be compared to "primary" and "secondary" consolidation respectively. The slopes on the log $\frac{de}{dt}$ - log t plot for each stage were found to be constant.

Three series of consolidation tests were performed to evaluate individually the effects of sample height, applied stress and initial void-ratio. In each of these series, two parameters were kept constant while the other parameter was varied over a suitable range. It was shown that the initial rate of consolidation (at t=1) is a function of sample height, applied stress and initial void-ratio. It was also shown that the time to the end of "Early-Stage" consolidation is a function of these three parameters.

In the third series of tests the samples had varying initial void-ratios, while the height and stress were held constant. The rates of consolidation were the same for all samples at any time in the "Late-Stage" consolidation (Fig. 11). This indicates that the initial void-ratio affects only the consolidation in the "Early-Stage" and not the consolidation in the "Late-Stage".

According to this pattern of peat consolidation, a nomograph with two sets of parallel lines in the log $\frac{de}{dt}$ - log t plot was constructed. By calculating the initial rate of consolidation and the time to the end of "Early-Stage" consolidation, the rate of consolidation at any time was determined by means of this nomograph. The total settlement can be established by integrating the consolidation rate equation for any time interval. This analysis has been proved to be valid for an amorphous-granular peat. If the approach can be shown to be valid for other peats as well, then six consolidation tests (varying the parameters H_i, σ, and e_i) are adequate for a consolidation analysis for a given peat type.

The consolidation tests in the laboratory were terminated after the s-log t curve became concave upward. Long term tests are needed to confirm that the slopes (k_2) on the log $\frac{de}{dt}$ - log t plot in the "Late-Stage" consolidation remain constant. The effects due to change in temperature and atmospheric pressure are significant compared with the low rate of consolidation in "Late-Stage" consolidation. It is recommended; therefore, that any long term consolidation tests be carried out in a constant temperature - pressure room.

In the consolidation tests, maximum pore-water pressures were not generated immediately after the load was applied as would be expected from Terzaghi's theory. Furthermore, in all the tests conducted, the pore-water pressures remained at substantial values at the point of 100% "primary" consolidation calculated from the Casagrande fitting method. Theoretically the pore-water pressure should have dissipated to almost zero at the point of 100% "primary" consolidation. These discrepencies may be due to time lag in the instrument or characteristics of this peat.

It is suggested that a three-dimensional consolidation test should be conducted for this soil from a slurry condition, with a specially designed three-dimensional consolidation. Earth pressure at rest, k_o, can be evaluated from this test. The flow characteristics of the soil under high stresses can also be studied.

The composition and structure of peat varies widely due to the difference of formation and age. Therefore, individual investigations of consolidation characteristics are necessary to determine if this approach is valid for different types of peat.

If the approach proves valid numerical k values can be established for different types of peat. A relationship between the k values and the types of peat (or the amount of organic content) is necessary to enable the prediction of settlements.

APPENDIX I

Evaluation of Frictional Resistance of the O-Rings on the Aluminum Cylinder Wall

In order to minimize leakage of the sample by the piston during consolidation, the piston was fitted with two O-rings. To obtain the net applied load on the sample, the frictional resistance of the O-rings on the aluminum cylinder wall was deducted from the total applied load.

In evaluating the frictional resistance of the O-rings on the aluminum cylinder wall, the consolidometer was mounted in a testing machine and the piston was moved downward. Frictional resistance was obtained at various rates. Frictional resistance was taken for three cases, i.e., O-rings dry, O-rings lubricated with tap water and lubricated with peat water. The results are shown in Fig. 19.

APPENDIX II

Evaluation of C_1, C_2 and t_f

From Fig. 13A, the relation between C_1, the initial rate of consolidation $\left[\left(\frac{dz}{dt}\right)_{t=1}\right]$ and H_1, sample height, can be written

$$\log \left(\frac{dz}{dt}\right)_{t=1} = \log C_1 = f_1(H_1) = a_1 + bH_1, \text{ for P I tests} \quad (1)$$

Similarly from Fig. 13A and Fig. 13C

$$\log \left(\frac{dz}{dt}\right)_{t=1} = \log C_1 = f_2(\sigma) = a_2 + c \log \sigma, \text{ for P II tests} \quad (2)$$

$$\log \left(\frac{dz}{dt}\right)_{t=1} = \log C_1 = f_3(e_1) = a_3 + d \log e_1, \text{ for P III tests} \quad (3)$$

Combining (1), (2) and (3),

$$\log \left(\frac{dz}{dt}\right)_{t=1} = \log C_1 = F(H_1, \sigma, e_1)$$

$$= a' + b'H_1 + c' \log \sigma + d' \log e_1$$

$$\log \left(\frac{dz}{dt}\right)_{t=1} = (a' + b'H_1) + \log (\sigma^{c'} * e_1^{d'})$$

$$\log \left[\left(\frac{dz}{dt}\right)_{t=1} / \sigma^{c'} \cdot e_1^{d'}\right] = (a' + b'H_1)$$

Therefore $C_1 = \left(\frac{dz}{dt}\right)_{t=1} = \sigma^{c'} \cdot e_1^{d'} \cdot 10^{(a'+b'H_1)}$ (4)

Substituting test data of P I, P II and P III tests, in which two of the parameters H_1, σ, e_1 were constant, allow the evaluation of the other parameter. The final result can be expressed

$$C_1 = \left(\frac{dz}{dt}\right)_{t=1} = \frac{\sigma^{0.34} \; e_1^{2.07}}{10^{(2.63 + 0.17 H_1)}}$$

By using the same procedures, C_2 and t_f can be evaluated.

NOTATIONS

C_1 - Initial rate, $(\frac{de}{dt})_{t=1}$, of "Early-Stage" consolidation

C_2 - Initial rate, $(\frac{de}{dt})_{t=1}$, of "Late-Stage" consolidation

e - Average void-ratio

e_i - Initial void-ratio

e_f - Final void-ratio

G - Specific gravity

H_i - Sample height (initial)

H_f - Final sample height

k_1 - Slope of straight line portion for "Early-Stage" consolidation in $\log \frac{de}{dt}$ - log t plot.

k_2 - Slope of straight line portion for "Late-Stage" consolidation in $\log \frac{de}{dt}$ - log t plot.

S - Settlement

t - Elapsed time

t_1 - Time to 100% primary consolidation by Casagrande fitting method

t_t - Time to the "End of Early-Stage" consolidation

t_w - Time to dissipation of pore-water pressure to insignificant value

U - Pore-water pressure

w - Water content

σ - Applied Stress

e_i - Void-ratio at 100% primary consolidation by Casagrande fitting method

e_t - Void-ratio at the "End of Early-Stage" consolidation

REFERENCES

Abbott, M.B., (1960). "One dimensional consolidation of multilayered soils"; Geotechnique, Vol. X, p. 151.

Adams, J.I. (1961). "Laboratory compression tests on peat"; Proc. 7th Muskeg Research Conf., N.R.C., T.M. No. 71, p. 36.

Bishop, A.W. and Henkel, D.J. (1957). "The measurement of soil properties in the triaxial test"; Arnold, London, 1957.

Brawner, C.O. (1961). "The compressibility of peat with reference to the construction of a major highway in B.C."; Proc. 7th Muskeg Research Conf., N.R.C., T.M. No. 71, p. 204.

Buisman, A.S. (1936). "Results of long duration settlement test"; Proc. 1st Int. Conf. of Soil Mech., Vol. I, p. 103.

Casagrande, A. (1936). "The determination of the pre-consolidation load and its practical significance"; Proc. 1st Int. Conf. of Soil Mech., Vol. III, p. 66.

Edelman, T. (1948). "Stress-strain relations, consolidation"; Proc. 2nd Int. Conf. of Soil Mech., Vol. I, p. 30.

Enright, C.T. and Adams, J.I. (1963). "A comparison of field and laboratory consolidation measurements in peat"; Proc. 9th Muskeg Research Conf. (N.R.C. in press).

Govindo, N.S. and Balakrihna, H.A. (1961). "A laboratory pore pressure measuring device"; Proc. 5th Int. Conf. of Soil Mech., Vol. I, p. 305.

Habib, P. (1960). "Contribution à la mesure des pressures interstitielles"; Conf. on Pore pressure and Suction in soils, Butterworths, London, 1961, p. 17.

Hardy, R.M. (1955). "Engineering characteristics of western muskeg"; Proc. Western Muskeg Research Conf., N.R.C. T.M. No. 38, p. 14.

Hanrahan, E.T. (1954). "An investigation of some physical properties of peat"; Geotechnique, Vol. IV, p. 108.

Hansen, J.B. (1961). "A model law for simultaneous primary and secondary consolidation"; Proc. 5th Int. Conf. of Soil Mech., Vol. I, p. 133.

Koppejan, A.W. (1948). "A formula combining the Terzaghi load compressio relationship and the Buisman time effect"; Proc. 2nd Int. Conf. of Soil Mech., Vol II, p. 32.

Lake, J.R. (1960). "Pore pressure and settlement measurements during small-scale and laboratory experiments to determine the effectiveness of vertical sand drains in peat"; Conf. on Pore pressure and Suction in soils , Butterworth, London, 1961, P. 103.

Lake, J.R. (1961). "Investigations of the problem of constructing roads on peat in Scotland"; Proc. 7th Muskeg Research Conf., N.R.C., T.M. No. 71, p. 133.

Leonards, G.A. and Girault, P. (1961)."A study of the one-dimensional consolidation test"; Proc. 5th Int. Conf. of Soil Mech. Vol. I, p. 213.

Lo, K.Y. (1961 a). "Stress-strain relationship and pore water pressure characteristics of a normally consolidated clay"; Proc. 5th Int. Conf. of Soil Mech., Vol. I, p. 219.

Lo, K.Y. (1961 b). "Secondary compression of clay"; ASCE Soil Mech. and Found. Div., Aug. 1961, p. 61.

Miyakawa, I. (1959). "Soil engineering research on peaty alluvia"; Reports 1 to 3, N.R.C., T.T. No. 1081, 1962.

Miyakawa, I. (1959). "Some aspects of road construction over peaty or marshy areas in Hokkaido, with particular reference to filling methods"; Civil Eng. Research Inst., Hokkaido Development Bureau, Japan.

Nash, K.L. and Dixon, R.K. (1960). "The measurement of pore pressure in sand under rapid triaxial test"; Conf. on Pore pressure and Suction in Soil, Butterworths, London, 1961, p. 21.

Naylor, M. andDoran, M. (1948). "Precise determination of primary consolidation"; Proc. 2nd Int. Conf. of Soil Mech., Vol I, p. 34.

Newland, P.L. and Allely, B.H. (1960). "A study of the consolidation characteristics of a clay"; Geotechnique, Vol. X, p. 62.

Radforth, N.W. (1952). "Suggested classification of muskeg for the engineer"; The Engineering Journal, Vol. 35,, Nov. 1952, p. 1194.

Radforth, N.W. and MacFarlane, I.C. (1957). "Correlation of palaeobotanical and engineering studies of muskeg in Canada"; Proc. 4th Int. Conf. of Soil Mech., Vol. I. p. 93.

Radforth, N.W. (1961). "Distribution of organic terrain in northern Canada"; Proc. 7th Muskeg Research Conf., N.R.C. T.M. No. 71, p. 8.

Schroeder, J. and Wilson, N.E. (1962). "The analysis of secondary consolidation of peat"; Proc. 8th Muskeg Research Conf., N.R.C. T.M. No. 74., p. 130.

Skempton, A. W. (1954). "The pore pressure coefficients A and B"; Geotechnique, Vol. IV, p. 143.

Sulijc, L. (1957). "The analysis of the consolidation process by the isotaches method"; Proc. 4th Int. Conf. of Soil Mech., Vol I, p.200.

Tan, T. K. (1957). "One-dimensional problems of consolidation and secondary time effects"; Academia Sinica.

Tan, T. K. (1957). "Two-dimensional problems of settlements of clay layers due to consolidation and secondary time effects"; Academia Sinica.

Tan, T. K. (1957). "Three-dimensional theory on the consolidation and flow of clay layers"; Academia Sinica.

Tan, T. K. (1958). "Secondary time effects and consolidation of clays"; Academia Sinica.

Taylor, D. W. (1942). "Research on consolidation of clays"; Dept. of Civil and Sanitary Eng., M.I.T.

Terzaghi, K. (1925). "Erdbaumechanik"; Franz. F. Deuticke.

Terzaghi, K. (1943). "Theoretical soil mechanics"; Wiley, New York.

Wahls, H. E. (1962). "Analysis of primary and secondary consolidation"; ASCE Soil Mech. and Found. Div., Jan. 1962, p.207.

TABLE 1

Summary of P I Tests (For variation of H_i)

Sample Number	Height of Sample (in.)		Applied Stress (lb/in^2)	Void-Ratio		Maximum pore-water pressure (lb/in^2)	Time to the "End of Early-Stage" (min.)	Initial rate of "Early-Stage" (min^{-1})	Initial rate of "Late-Stage" (min^{-1})
	H_i	H_f	σ	e_i	e_f	U max.	t_t	C_1	C_2
P I 1	6.45	3.49	3.63	14.38	6.75	3.42	3,500	0.058	7.1×10^{7}
P I 2	5.94	3.19	3.63	14.45	7.36	1.74*	3,100	0.070	4.2×10^{7}
P I 3	3.66	1.81	3.63	14.64	6.74	3.06	720	0.175	1.1×10^{6}
P I 4	2.91	1.38	3.63	15.45	6.78	3.48	540	0.195	2.1×10^{5}
P I 5	1.88	0.95	3.63	15.80	7.45	3.10	220	0.320	5.5×10^{4}
P I 6	0.84	0.47	3.63	14.16	7.00	2.85	40	0.370	9.2×10^{3}
P I 7	0.74	0.37	3.63	14.40	6.82	3.43	20	0.580	6.8×10^{3}
P I 8	0.27	0.20	3.63	14.50	6.63	1.17**	3.5	0.770	3.8×10^{3}

* Due to leakage of manometer.

** This is not the maximum pore-water pressure; the pore-water pressure had dissipated by the time of first reading.

TABLE 2

Summary of P II tests (For variation of σ)

Sample Number	Applied Stress σ (lb/in^2)	Height of Sample (in.) H_i	H_f	Void-Ratio e_i	e_f	e_1	e_t	Time t_i	t_v	t_t	Maximum Pore-water Pressure (lb/in^2) U max.	Initial Rate of "Early-Stage" ($min.^{-1}$) C_1	Initial Rate of "Late-Stage" ($min.^{-1}$) C_2
P II 1	0.45	0.99	0.72	10.50	7.34	7.36	7.88	230	420	120	0.52	0.170	1.5×10^{-4}
P II 2	0.86	0.97	0.65	10.55	6.82	6.87	7.50	190	370	100	0.93	0.205	1.35×10^{-4}
P II 3	1.09	0.95	0.86	11.15	6.81	6.82	7.48	190	290	100	1.04	0.240	1.3×10^{-4}
P II 4	1.51	0.94	0.59	10.50	6.30	6.34	7.10	165	190	86	1.64	0.235	1.25×10^{-4}
P II 5	1.83	0.89	0.51	10.05	6.08	6.10	6.72	135	180	80	1.90	0.260	1.2×10^{-4}
P II 6	2.35	0.92	0.55	10.60	5.94	6.04	6.70	125	180	80	2.40	0.280	1.15×10^{-4}
P II 7	2.78	0.89	0.51	10.80	5.78	5.93	6.65	120	170	72	2.78	0.315	1.1×10^{-4}
P II 8	3.63	0.89	0.47	10.85	5.32	5.52	6.22	105	160	68	3.67	0.365	1.05×10^{-4}
P II 9	4.48	0.92	0.47	11.30	5.36	5.55	6.22	100	155	68	4.56	0.380	1.0×10^{-4}
P II 10	7.03	0.87	0.41	11.65	5.03	5.20	5.83	74	120	56	6.87	0.470	9.0×10^{-5}

TABLE 3

Summary of P III Tests (For variation of e_i)

Sample Number	Void-Ratio		Height of Sample (in.)		Applied Stress (lb/in^2)	Maximum pore-water pressure (lb/in^2)	Time to the "End of Early-Stage" (min.)	Initial rate of "Early-Stage" ($min.^{-1}$)	Initial rate of "Late-Stage" ($min.^{-1}$)
	e_1	e_2	H_1	H_2	σ	U max.	t_t	C_1	C_2
P III 1	12.40	5.54	0.93	0.45	3.63	3.58	72	0.360	1.5×10^{-4}
P III 2	11.80	5.42	0.92	0.51	3.63	3.56	74	0.340	1.5×10^{-4}
P.III 3	10.90	5.46	0.98	0.53	3.63	3.48	79	0.300	1.5×10^{-4}
P III 4	9.56	5.35	0.92	0.55	3.63	3.56	88	0.220	1.5×10^{-4}
P III 5	9.47	5.51	0.98	0.61	3.63	3.60	92	0.200	1.5×10^{-4}
P III 6	8.62	5.43	1.01	0.67	3.63	3.33	105	0.160	1.5×10^{-4}

TABLE 4

Analysis data for P II 1 Test (σ = 0.45 lb/in.^{2})

Time (min.)			Void-Ratio		Rate of Consolidation (min.$^{-1}$)	Pore-Water Pressure (lb/in.^{2})
t	t*	Δt	e	Δe	Δe/Δt	U
0			10.50			
	0.25	0.5		0.22	0.44	0.27
0.5			10.28			
	0.75	0.5		0.10	0.20	0.37
1			10.18			
	1.5	1		0.14	0.14	0.43
2			10.04			
	2.5	1		0.10	0.10	0.45
3			9.94			
	4	2		0.15	0.075	0.48
5			9.79			
	6	2		0.11	0.055	0.50
7			9.68			
	8.5	3		0.15	0.050	0.51
10			9.53			
	12.5	5		0.19	0.038	0.52
15			9.34			
	17.5	5		0.17	0.034	0.52
20			9.17			
	22.5	5		0.14	0.028	0.51
25			9.03			
	27.5	5		0.11	0.022	0.51
30			8.92			
	35	10		0.20	0.020	0.51
40			8.72			
	45	10		0.16	0.016	0.51
50			8.56			
	60	20		0.26	0.013	0.50
70			8.30			
	102.5	65		0.51	0.0078	0.43
135			7.79			
	195	120		0.31	0.0026	0.27
255			7.48			
	310	110		0.10	0.00091	0.17
365			7.38			
	442.5	155		0.04	0.00026	0.17
520			7.34			

t* is the time between two successive readings

TABLE 4 (Continued)

Analysis data for P II 2 test (σ = 0.86 lb/in.^{2})

Time (min.)			Void-Ratio		Rate of Consolidation (min.$^{-1}$)	Pore-Water pressure (lb/in.^{2})
t	t°	Δt	e	Δe	Δe/Δt	U
0			10.55			
	0.25	0.5		0.33	0.66	0.70
0.5			10.22			
	0.75	0.5		0.11	0.22	0.77
1			10.11			
	1.5	1		0.17	0.17	0.83
2			9.95			
	2.5	1		0.12	0.12	0.87
3			9.82			
	4	2		0.19	0.095	0.89
5			9.63			
	6	2		0.14	0.070	0.91
7			9.49			
	8.5	3		0.17	0.056	0.91
10			9.32			
	12.5	5		0.23	0.046	0.93
15			9.09			
	17.5	5		0.19	0.038	0.93
20			8.90			
	22.5	5		0.16	0.032	0.93
25			8.74			
	27.5	5		0.14	0.028	0.93
30			8.60			
	35	10		0.25	0.025	0.92
40			8.35			
	45	10		0.20	0.020	0.91
50			8.15			
	60	20		0.33	0.016	0.87
70			7.82			
	85	30		0.34	0.011	0.79
100			7.48			
	137.5	75		0.40	0.0053	0.58
175			7.08			
	220	95		0.16	0.0017	0.31
265			6.92			
	295	65		0.04	0.00062	0.25
325			6.88			
	520	390		0.06	0.00015	0.23
715			6.82			

TABLE 4 (Continued)

Analysis data for P II 3 test (σ = 1.09 lb/in.^{2})

Time			Void-Ratio		Rate of Consolidation (min.$^{-1}$)	Pore-Water Pressure (lb/in.^{2})
t	t*	Δt	e	Δe	Δe/Δt	U
0			11.15			
	0.25	0.5		0.23	0.46	1.04
0.5			10.92			
	0.75	0.5		0.13	0.26	1.04
1			10.79			
	1.5	1		0.19	0.19	1.04
2			10.60			
	2.5	1		0.13	0.13	1.04
3			10.47			
	4	2		0.22	0.11	1.04
5			10.25			
	6	2		0.15	0.075	1.04
7			10.10			
	8.5	3		0.20	0.067	1.04
10			9.90			
	12.5	5		0.27	0.054	1.04
15			9.63			
	17.5	5		0.21	0.042	1.04
20			9.42			
	22.5	5		0.19	0.038	1.04
25			9.23			
	27.5	5		0.16	0.032	1.03
30			9.07			
	35	10		0.30	0.030	1.02
40			8.77			
	45	10		0.23	0.023	1.01
50			8.54			
	60	20		0.44	0.022	0.94
70			8.10			
	85	30		0.61	0.020	0.81
100			7.49			
	135	70		0.45	0.0064	0.53
170			7.04			
	215	90		0.16	0.0017	0.12
260			6.88			
	290	60		0.04	0.00067	0.06
320			6.84			
	365	90		0.03	0.00033	0.06
410			6.81			

TABLE 4 (Continued)

Analysis data for P II 4 test (σ = 1.51 lb/in.^{2})

Time			Void-Ratio		Rate of Consolidation (min.$^{-1}$)	Pore-Water Pressure (lb/in.^{2})
t	t°	Δt	e	Δe	Δe/Δt	U
0			10.50			
	0.25	0.5		0.16	0.32	1.64
0.5			10.34			
	0.75	0.5		0.15	0.30	1.64
1			10.19			
	1.5	1		0.21	0.21	1.64
2			9.98			
	2.5	1		0.14	0.14	1.64
3			9.84			
	4	2		0.21	0.11	1.63
5			9.63			
	6	2		0.17	0.085	1.63
7			9.46			
	8.5	3		0.21	0.070	1.63
10			9.25			
	12.5	5		0.28	0.056	1.63
15			8.97			
	17.5	5		0.23	0.046	1.63
20			8.74			
	22.5	5		0.20	0.040	1.62
25			8.54			
	27.5	5		0.17	0.034	1.61
30			8.37			
	35	10		0.32	0.032	1.59
40			8.05			
	45	10		0.27	0.027	1.54
50			7.78			
	55	10		0.23	0.023	1.46
60			7.55			
	82.5	45		0.68	0.015	1.12
105			6.87			
	127.5	45		0.27	0.0060	0.58
150			6.60			
	187.5	75		0.18	0.0024	0.29
225			6.42			
	252.5	55		0.04	0.00073	0.23
280			6.38			
	320	80		0.04	0.00050	0.21
360			6.34			
	465	210		0.04	0.00019	0.17
570			6.30			

TABLE 4 (Continued)

Analysis data for P II 5 Test (σ = 1.83 lb/in.^{2})

Time			Void-Ratio		Rate of Consolidation (min.$^{-1}$)	Pore-Water Pressure (lb/in.^{2})
t	t*	Δt	e	Δe	Δe/Δt	U
0			10.05			
	0.25	0.5		0.30	0.60	1.85
0.5			9.75			
	0.75	0.5		0.12	0.24	1.87
1			9.63			
	1.5	1		0.18	0.18	1.90
2			9.45			
	2.5	1		0.14	0.14	1.90
3			9.31			
	4	2		0.20	0.10	1.90
5			9.11			
	6	2		0.19	0.095	1.90
7			8.92			
	8.5	3		0.20	0.066	1.90
10			8.72			
	12.5	5		0.28	0.056	1.90
15			8.44			
	17.5	5		0.24	0.048	1.90
20			8.20			
	22.5	5		0.18	0.036	1.90
25			8.02			
	27.5	5		0.17	0.034	1.90
30			7.85			
	35	10		0.30	0.030	1.87
40			7.55			
	45	10		0.27	0.027	1.80
50			7.28			
	60	20		0.39	0.019	1.55
70			6.89			
	92.5	45		0.51	0.011	1.00
115			6.38			
	137.5	45		0.16	0.0036	0.45
160			6.22			
	197.5	75		0.10	0.0013	0.17
235			6.12			
	262.5	55		0.02	0.00036	0.10
290			6.10			
	330	80		0.02	0.00025	0.08
370			6.08			

TABLE 4 (Continued)

Analysis data for P II 6 test (σ= 2.35 lb/in.^{2})

Time (min.)			Void-Ratio		Rate of Consolidation (min.$^{-1}$)	Pore-Water Pressure (lb/in.^{2})
t	t*	Δt	e	Δe	Δe/Δt	U
0			10.60			
	0.25	0.5		0.25	0.50	2.32
0.5			10.35			
	0.75	0.5		0.17	0.34	2.34
1			10.18			
	1.5	1		0.23	0.23	2.36
2			9.95			
	2.5	1		0.16	0.16	2.38
3			9.79			
	4.0	2		0.24	0.12	2.39
5			9.55			
	6.0	2		0.19	0.095	2.39
7			9.36			
	8.5	3		0.26	0.087	2.39
10			9.10			
	12.5	5		0.34	0.068	2.39
15			8.76			
	17.5	5		0.28	0.056	2.38
20			8.48			
	22.5	5		0.25	0.050	2.36
25			8.23			
	27.5	5		0.22	0.044	2.32
30			8.01			
	35	10		0.37	0.037	2.24
40			7.64			
	45	10		0.34	0.034	2.09
50			7.30			
	60	20		0.46	0.023	1.82
70			6.84			
	90	40		0.49	0.012	1.20
110			6.35			
	140	60		0.25	0.0042	0.43
170			6.10			
	200	60		0.10	0.0017	0.25
230			6.00			
	270	80		0.03	0.00037	0.17
310			5.97			
	360	100		0.03	0.00033	0.15
410			5.94			

TABLE 4 (Continued)

Analysis data for P II 7 test (σ = 2.78 lb/in.^{2})

Time (min.)			Void-Ratio		Rate of Consolidation (min.$^{-1}$)	Fore-Water Pressure (lb/in.^{2})
t	t*	Δt	e	Δe	$\Delta e/\Delta t$	U
0			10.80			
	0.25	0.5		0.24	0.48	2.76
0.5			10.56			
	0.75	0.5		0.14	0.28	2.77
1			10.42			
	1.5	1		0.24	0.24	2.78
2			10.18			
	2.5	1		0.17	0.17	2.78
3			10.01			
	4	2		0.28	0.14	2.78
5			9.73			
	6	2		0.21	0.11	2.78
7			9.52			
	8.5	3		0.29	0.097	2.78
10			9.23			
	12.5	5		0.40	0.080	2.77
15			8.83			
	17.5	5		0.30	0.060	2.75
20			8.53			
	22.5	5		0.27	0.054	2.71
25			8.26			
	27.5	5		0.24	0.048	2.67
30			8.02			
	35	10		0.41	0.041	2.59
40			7.61			
	45	10		0.34	0.034	2.48
50			7.27			
	60	20		0.52	0.026	2.24
70			6.75			
	95	50		0.63	0.013	1.35
120			6.12			
	150	60		0.20	0.0033	0.43
180			5.92			
	210	60		0.09	0.0015	0.17
240			5.83			
	280	80		0.05	0.00037	0.08
320			5.80			
	370	100		0.02	0.00020	0.08
420			5.78			

TABLE 4 (Continued)

Analysis data for P II 8 test (σ= 3.63 lb/in.^{2})

Time (min.)			Void-Ratio		Rate of Consolidation (min.$^{-1}$)	Pore-Water Pressure (lb/in.^{2})
t	t'	Δt	e	Δe	Δe/Δt	U
0			10.85			
	0.25	0.5		0.35	0.70	3.58
0.5			10.50			
	0.75	0.5		0.17	0.34	3.58
1			10.33			
	1.5	1		0.26	0.26	3.60
2			10.07			
	2.5	1		0.21	0.21	3.64
3			9.86			
	4	2		0.33	0.16	3.63
5			9.53			
	6	2		0.26	0.13	3.65
7			9.27			
	8.5	3		0.32	0.11	3.67
10			8.95			
	12.5	5		0.43	0.086	3.64
15			8.52			
	17.5	5		0.34	0.068	3.60
20			8.18			
	22.5	5		0.34	0.068	3.54
25			7.84			
	27.5	5		0.27	0.054	3.48
30			7.58			
	35	10		0.47	0.047	3.33
40			7.10			
	45	10		0.37	0.037	3.13
50			6.73			
	60	20		0.55	0.027	2.67
70			6.18			
	90	40		0.53	0.013	1.55
110			5.65			
	125	30		0.16	0.0053	0.77
140			5.49			
	170	60		0.11	0.0018	0.30
200			5.38			
	235	70		0.06	0.00086	0.23
270			5.32			

TABLE 4 (Continued)

Analysis of data for C II 9 test (σ = 4.48 lb/in.^{2})

Time (min.)			Void-Ratio		Rate of Consolidation (min.$^{-1}$)	Pore-Water Pressure (lb/in.^{2})
t	t'	Δt	e	Δe	Δe/Δt	U
0			11.30			
	0.25	0.5		0.50	1.00	4.16
0.5			10.80			
	0.75	0.5		0.20	0.40	4.41
1			10.60			
	1.5	1		0.30	0.30	4.51
2			10.30			
	2.5	1		0.23	0.23	4.56
3			10.07			
	4	2		0.32	0.16	4.56
5			9.75			
	6	2		0.28	0.14	4.56
7			9.47			
	8.5	3		0.36	0.12	4.55
10			9.11			
	12.5	5		0.45	0.090	4.51
15			8.66			
	17.5	5		0.40	0.080	4.46
20			8.26			
	22.5	5		0.33	0.066	4.39
25			7.93			
	27.5	5		0.29	0.058	4.31
30			7.64			
	35	10		0.48	0.048	4.16
40			7.16			
	45	10		0.39	0.039	3.93
50			6.77			
	60	20		0.59	0.029	3.19
70			6.18			
	80	20		0.31	0.015	2.28
90			5.87			
	105	30		0.25	0.0083	1.45
120			5.62			
	135	30		0.12	0.0040	0.81
150			5.50			
	180	60		0.08	0.0013	0.35
210			5.42			
	245	70		0.06	0.00086	0.10
280			5.36			

TABLE 4 (Continued)

Analysis data for P II 10 test (σ = 7.03 lb/in.^{2})

Time (min.)			Void-Ratio		Rate of Consolidation (min.$^{-1}$)	Pore-Water Pressure (lb/in.^{2})
t	t'	Δt	e	Δe	Δe/Δt	U
0			11.65			
	0.25	0.5		0.67	1.34	6.29
0.5			10.98			
	0.75	0.5		0.26	0.52	6.52
1			10.72			
	1.5	1		0.36	0.36	6.72
2			10.36			
	2.5	1		0.29	0.29	6.81
3			10.07			
	4	2		0.45	0.22	6.87
5			9.62			
	6	2		0.34	0.17	6.87
7			9.28			
	8.5	3		0.40	0.13	6.81
10			8.88			
	12.5	5		0.55	0.11	6.77
15			8.33			
	17.5	5		0.46	0.092	6.68
20			7.87			
	22.5	5		0.43	0.085	6.39
25			7.44			
	27.5	5		0.38	0.076	6.29
30			7.06			
	35	10		0.62	0.062	5.66
40			6.44			
	45	10		0.40	0.040	4.84
50			6.04			
	60	20		0.46	0.023	3.48
70			5.58			
	85	30		0.30	0.010	1.64
100			5.28			
	120	40		0.13	0.0032	0.62
140			5.15			
	190	100		0.09	0.00090	0.19
240			5.06			
	270	60		0.03	0.00050	0.14
300			5.03			

FIGURES

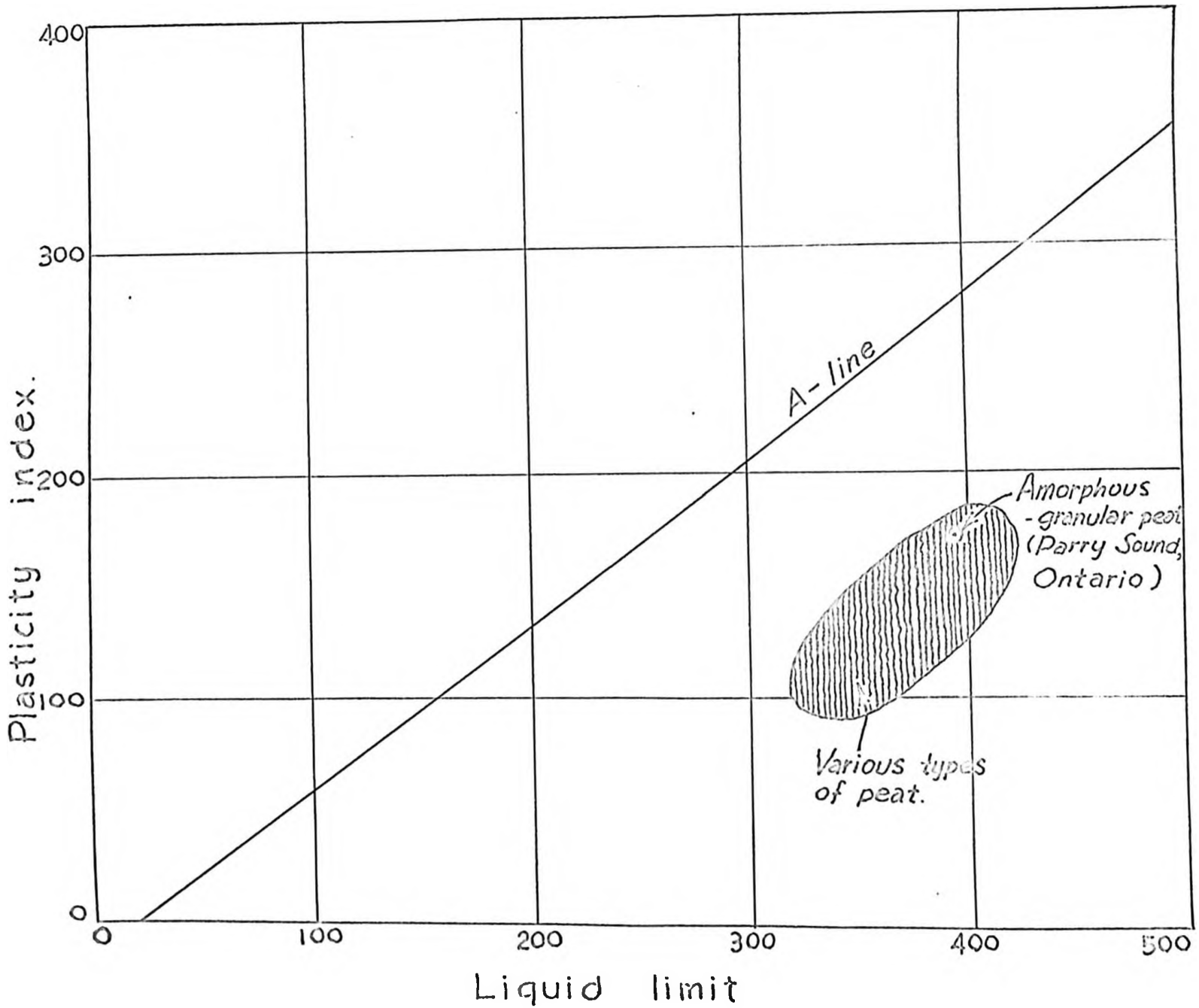

Fig. 1. Plasticity chart (after Casagrande).

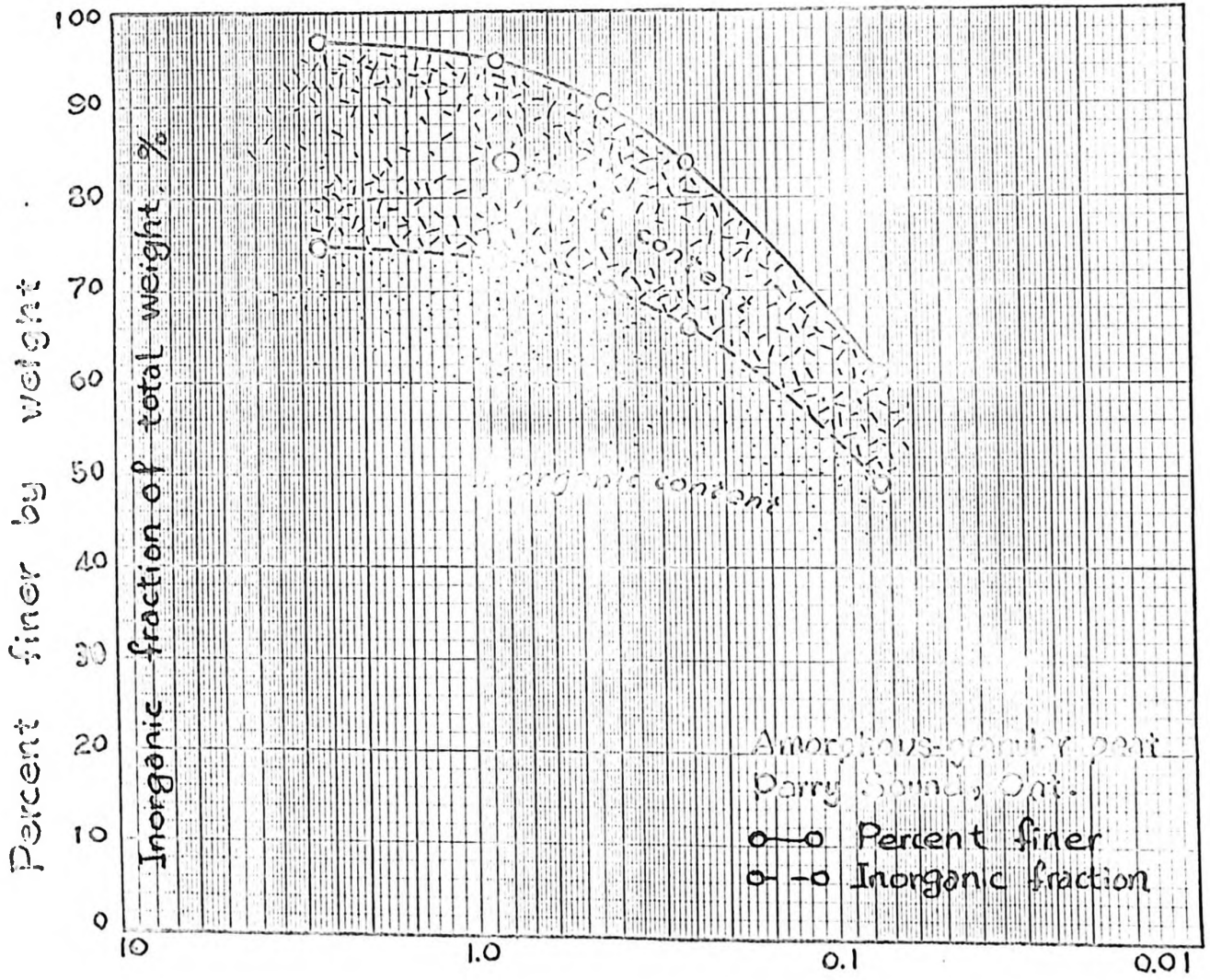

"Equivalent" particle diameter, (mm)

Fig.2. Particle size and organic content of amorphous-granular peat.

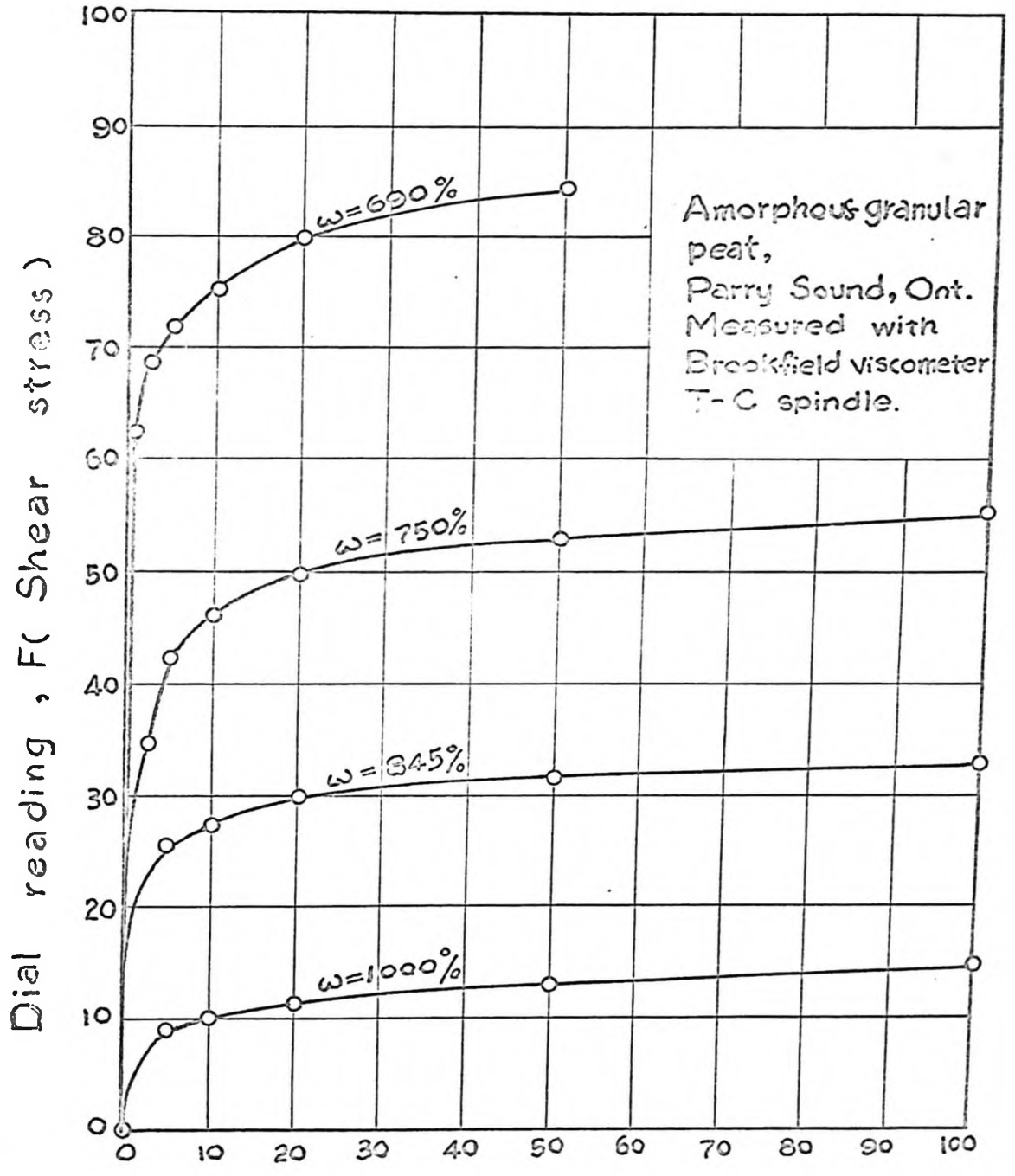

Fig. 3. Rheological diagram.

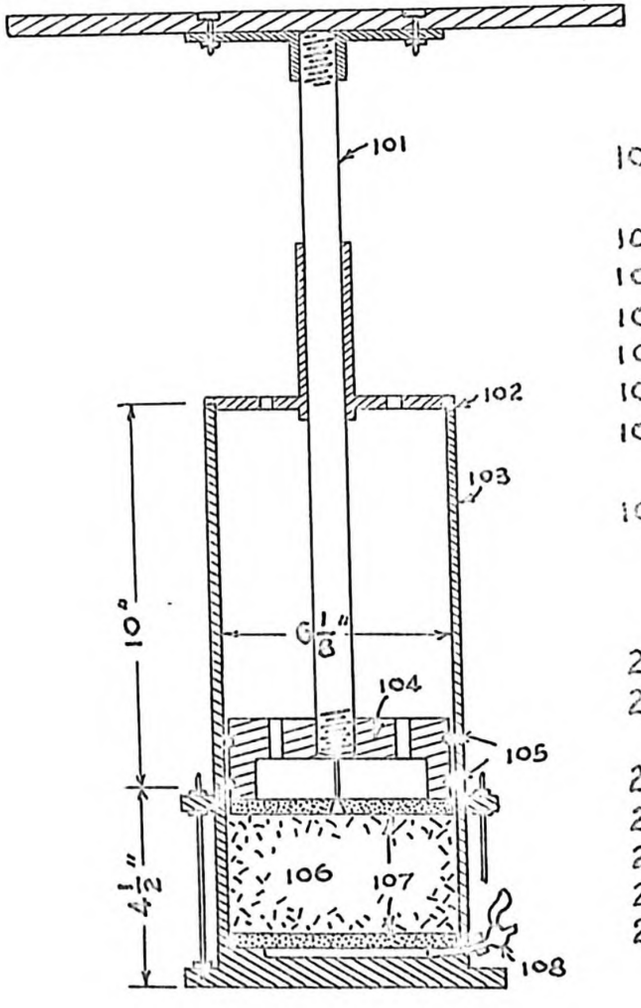

101 Hollow aluminum shaft.
102 Over flow hole.
103 Aluminum cylinder.
104 Piston.
105 O-rings.
106 Sample
107 P2120 Norton porous stone.
108 Valve in connection with manometer.

201 Air release valve.
202 Connection to consolidometer
203 1 mm I.D. glass tubing
204 Distilled water
205 Mercury
206 Scale
207 24 mm I.D glass bulb.

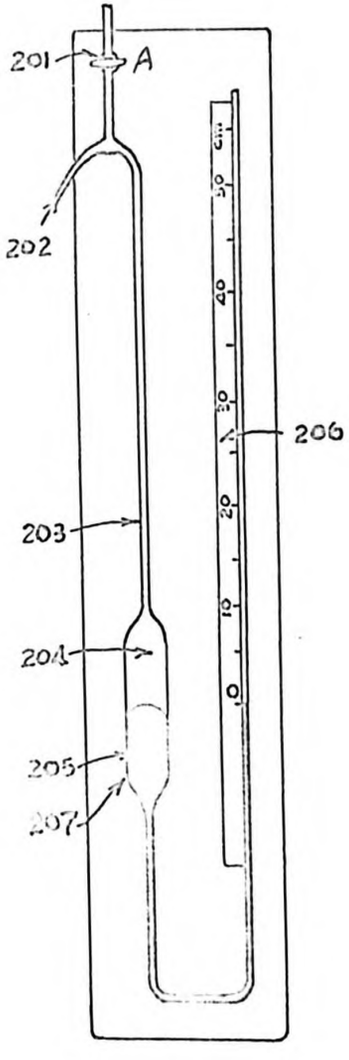

Consolidometer

Manometer board

Fig. 4. Consolidometer and Manometer board.

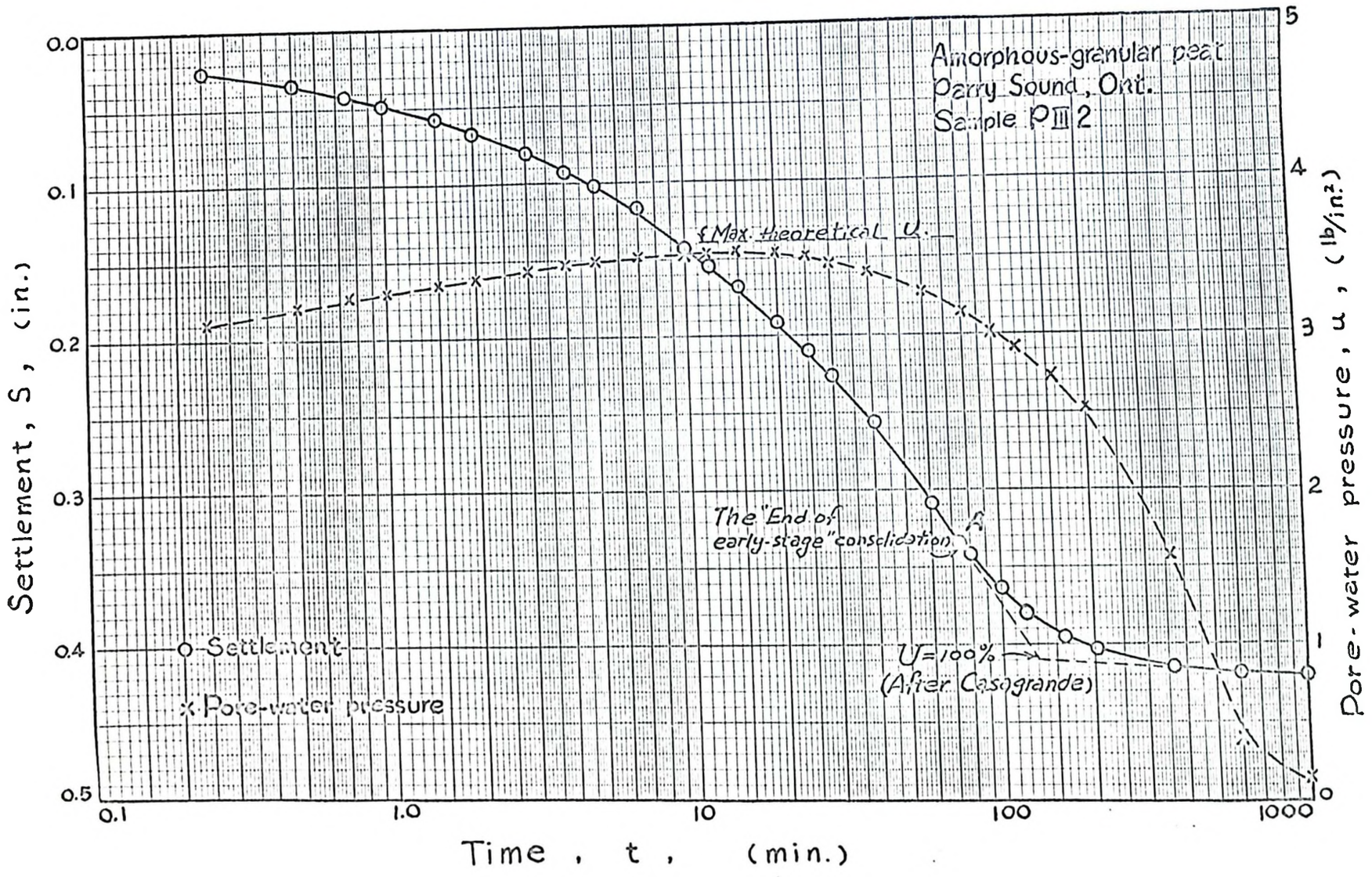

Fig.5. Typical curves of settlement and pore-water pressure versus time.

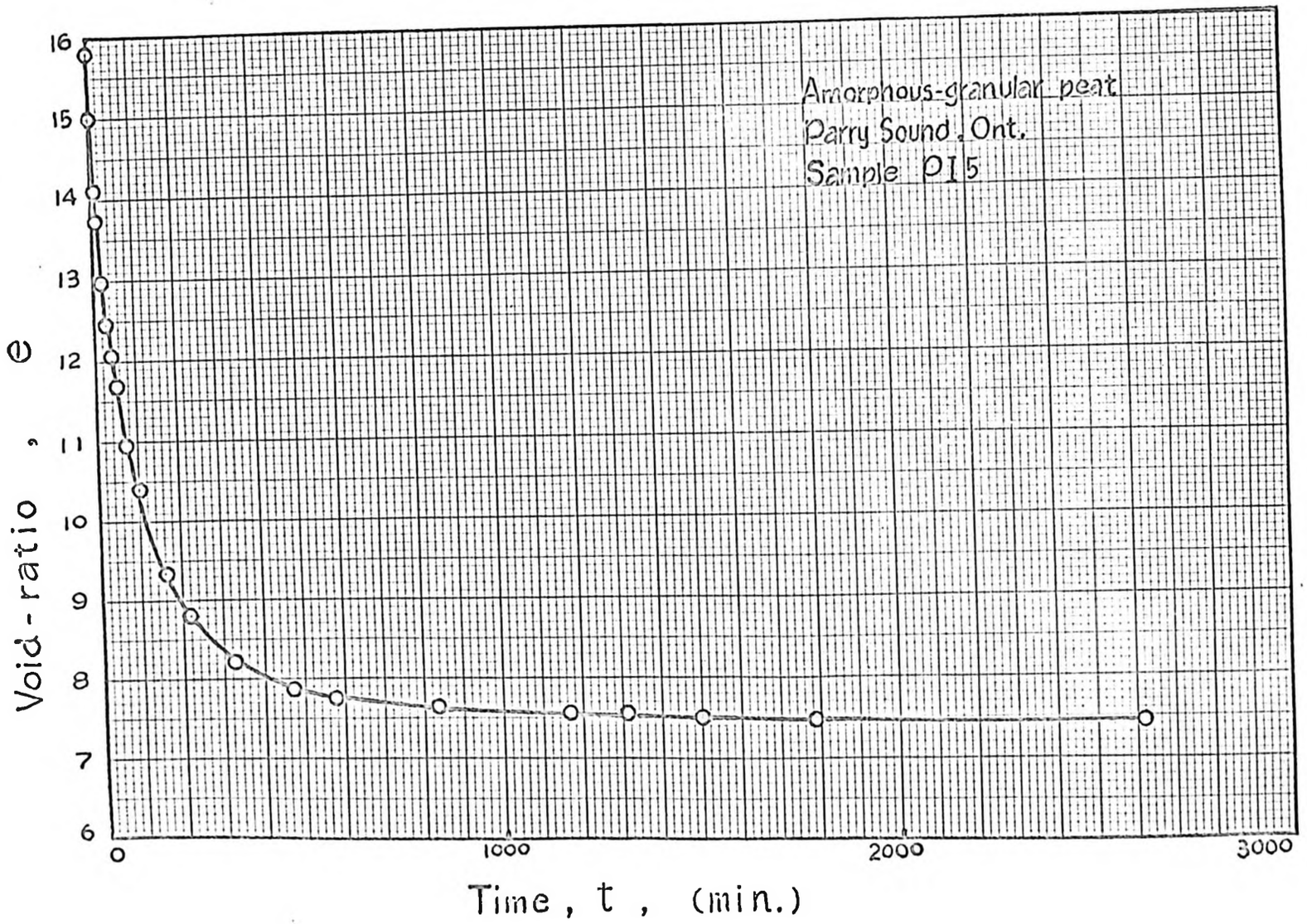

Fig. 6. Typical void-ratio — time curve.

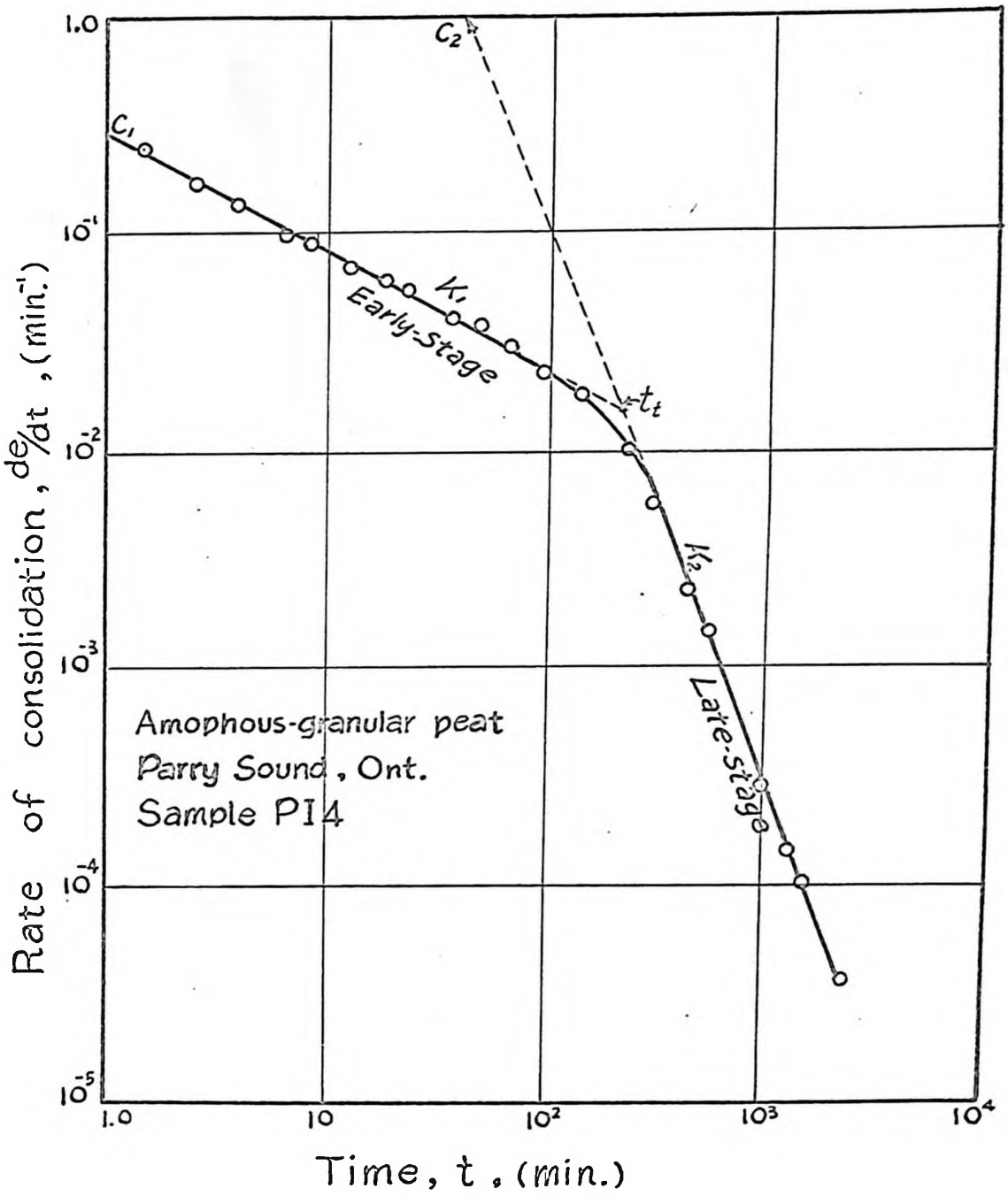

Fig.7. Typical curve of rate of consolidation versus time.

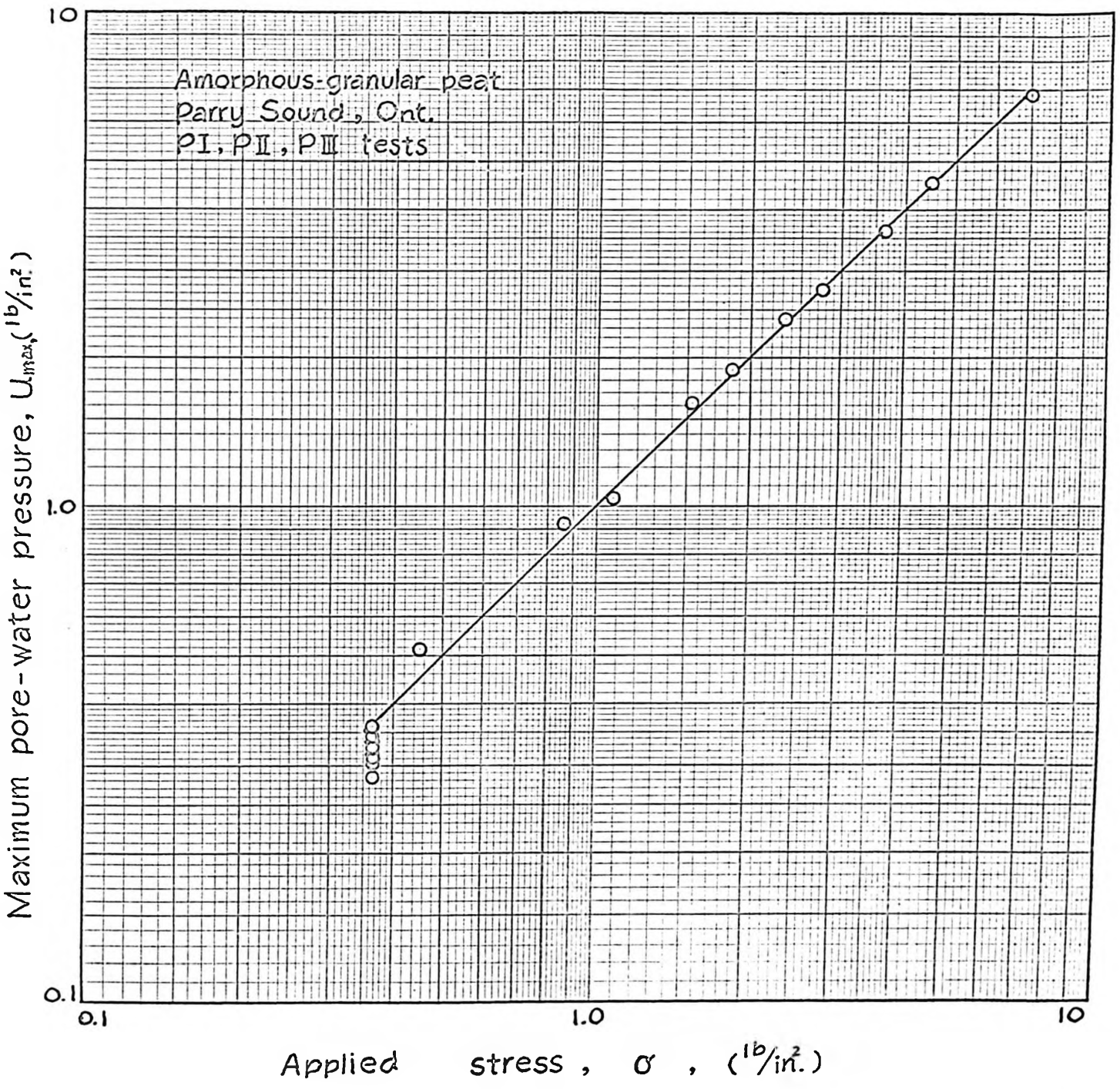

Fig.8. Maximum pore-water pressure versus applied stress.

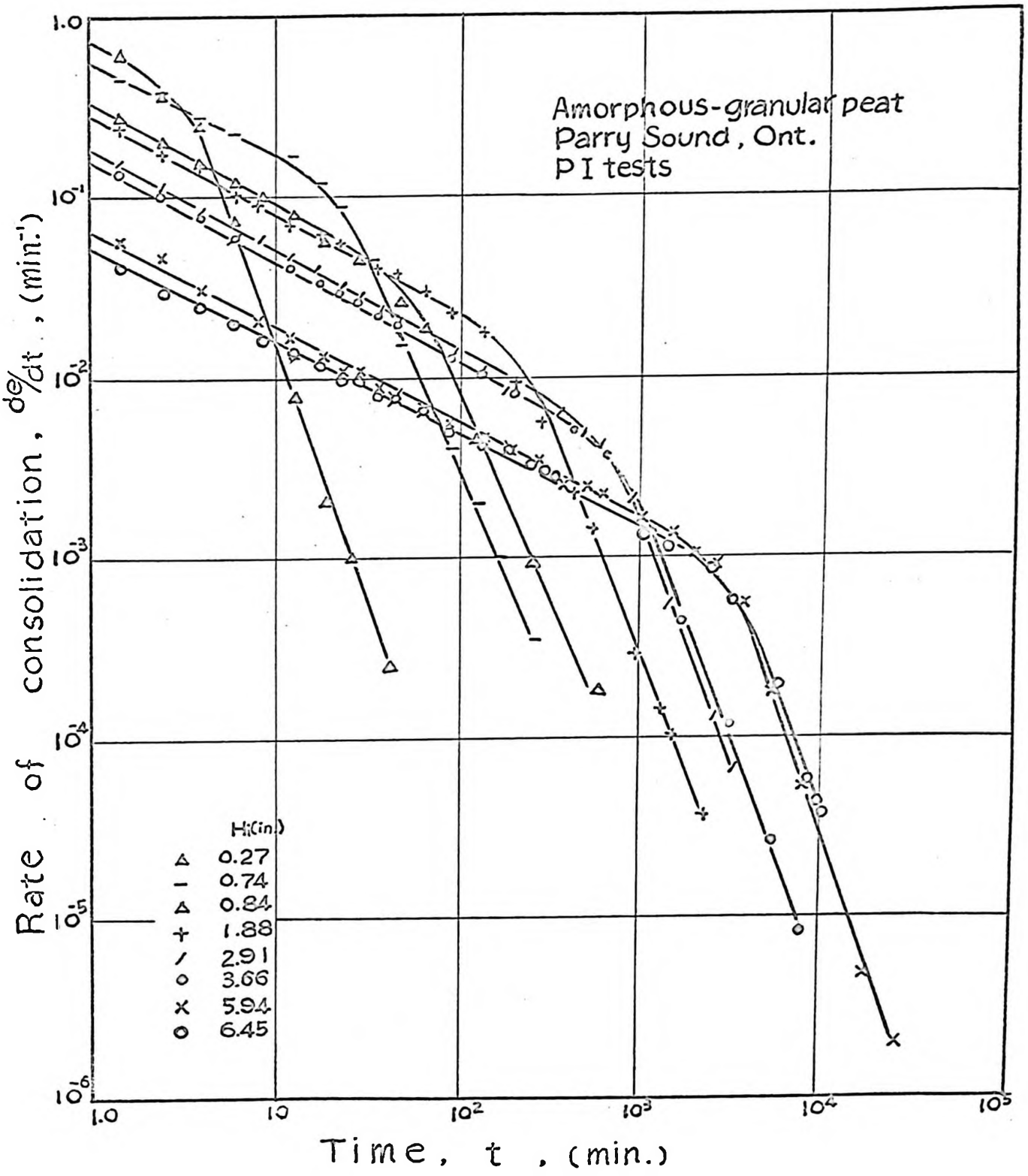

Fig.9. Rate of consolidation versus time for samples of various heights.

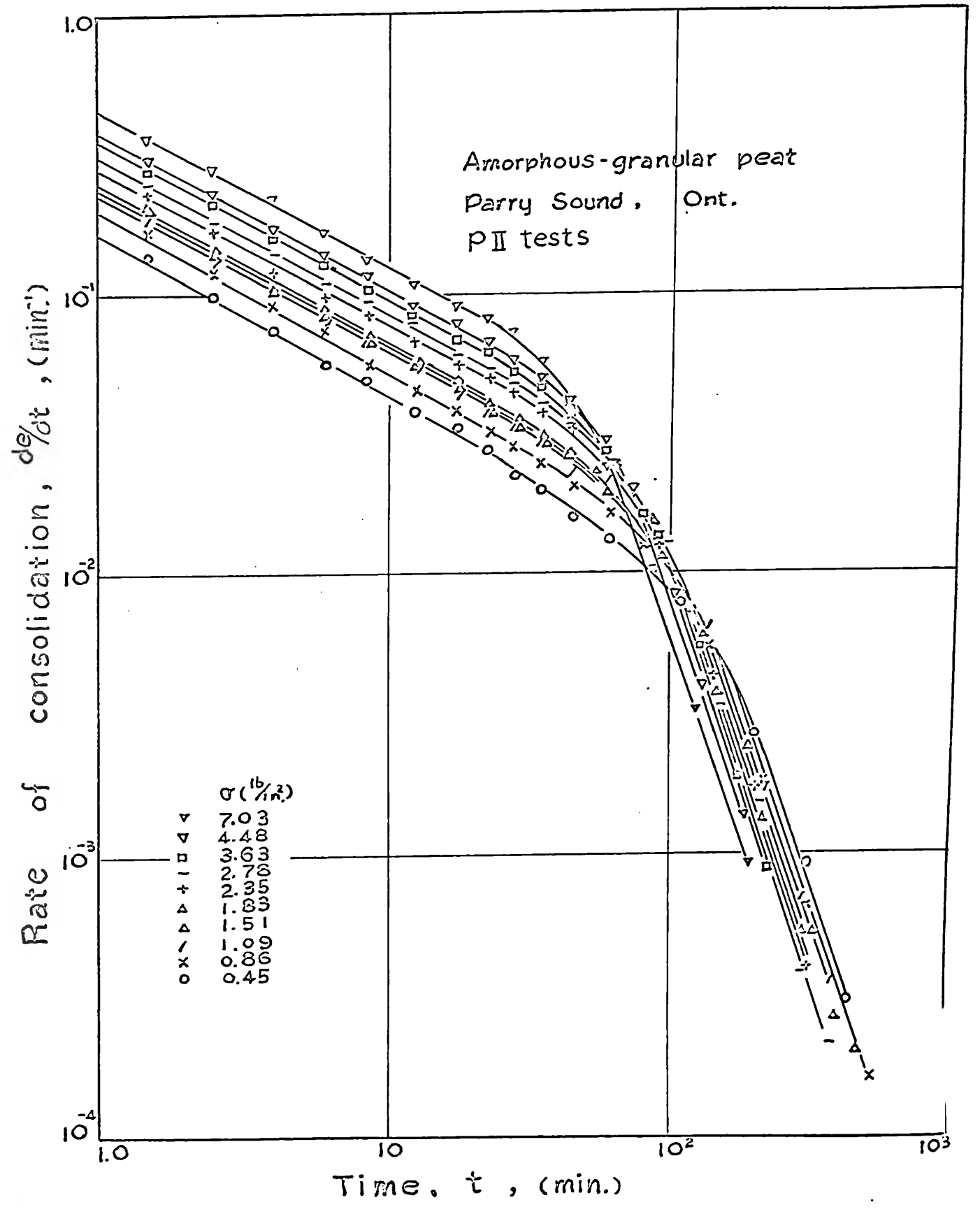

Fig.10. Rate of consolidation versus time for samples under various stresses.

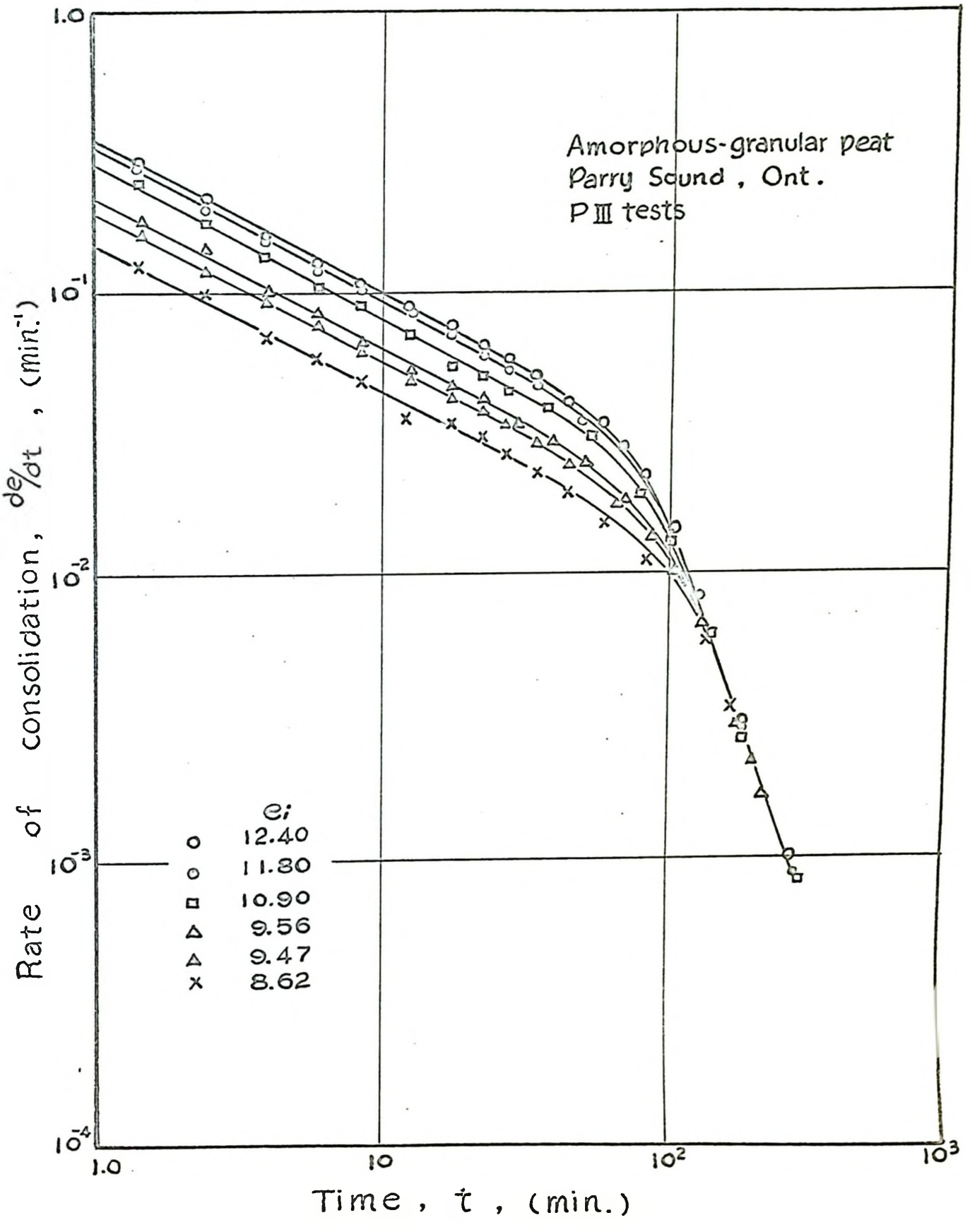

Fig.11. Rate of consolidation versus time for samples of various initial void-ratios.

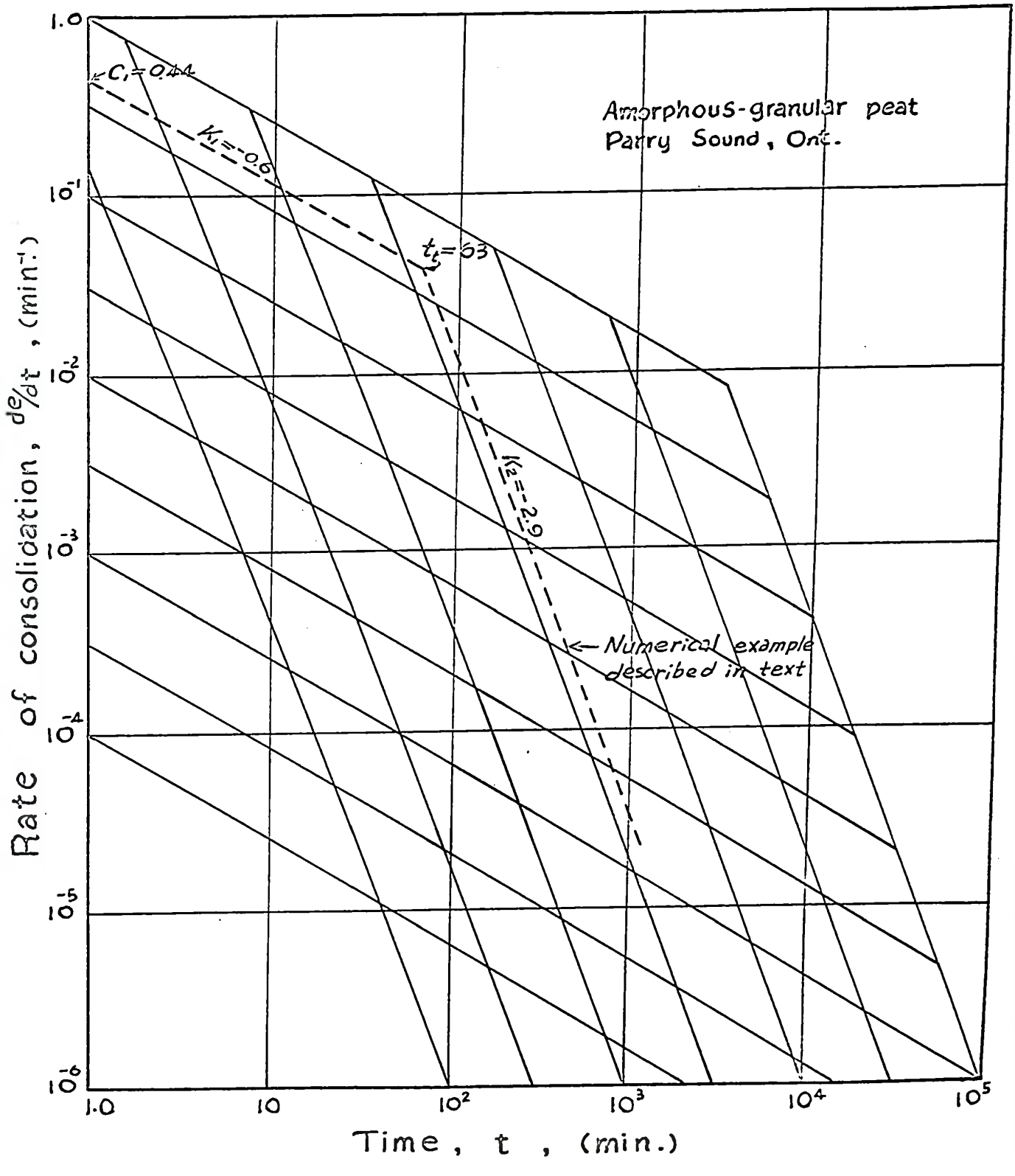

Fig.12. Nomograph to predict the rate of consolidation.

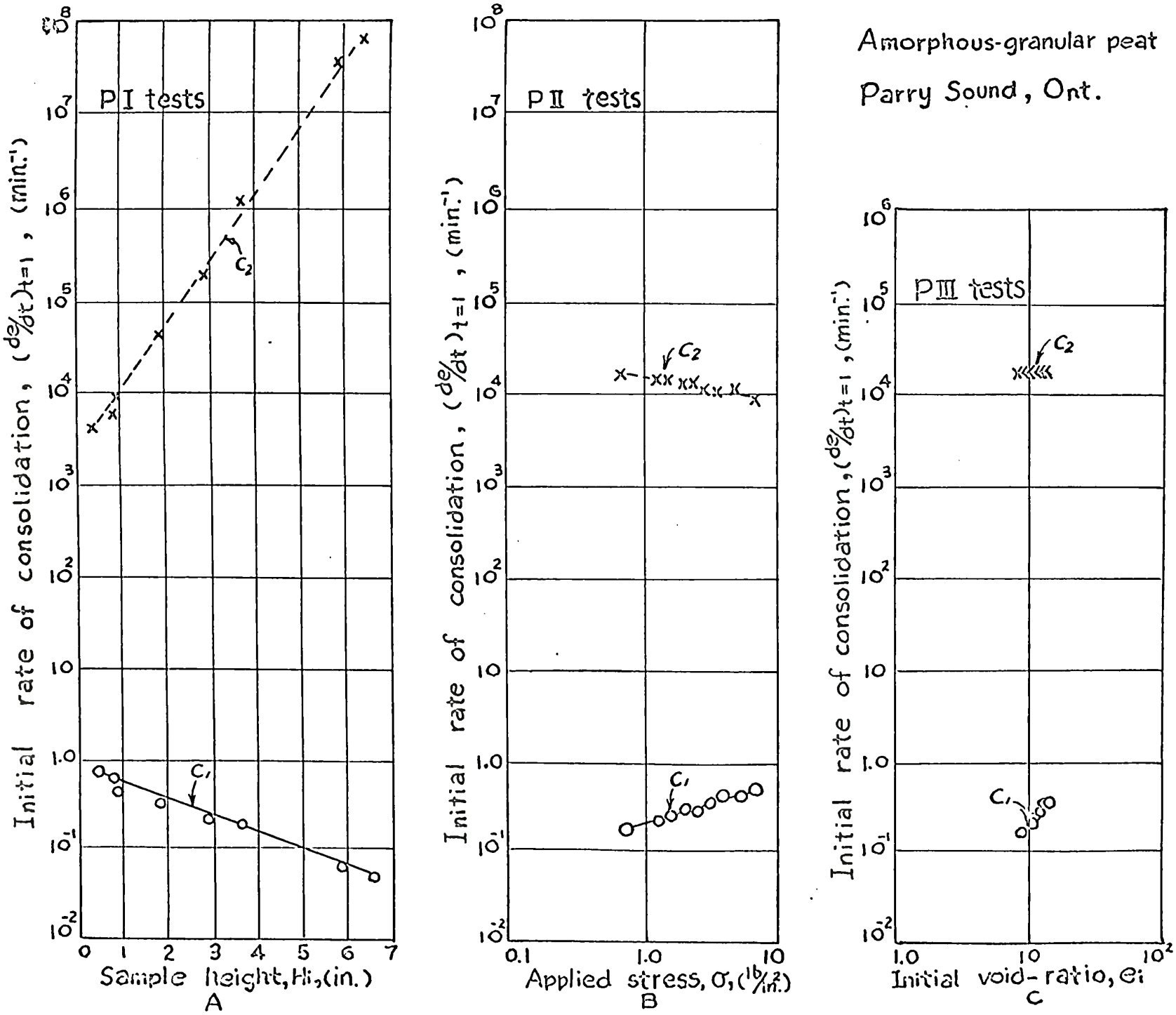

Fig. 13. Initial rates of consolidation.

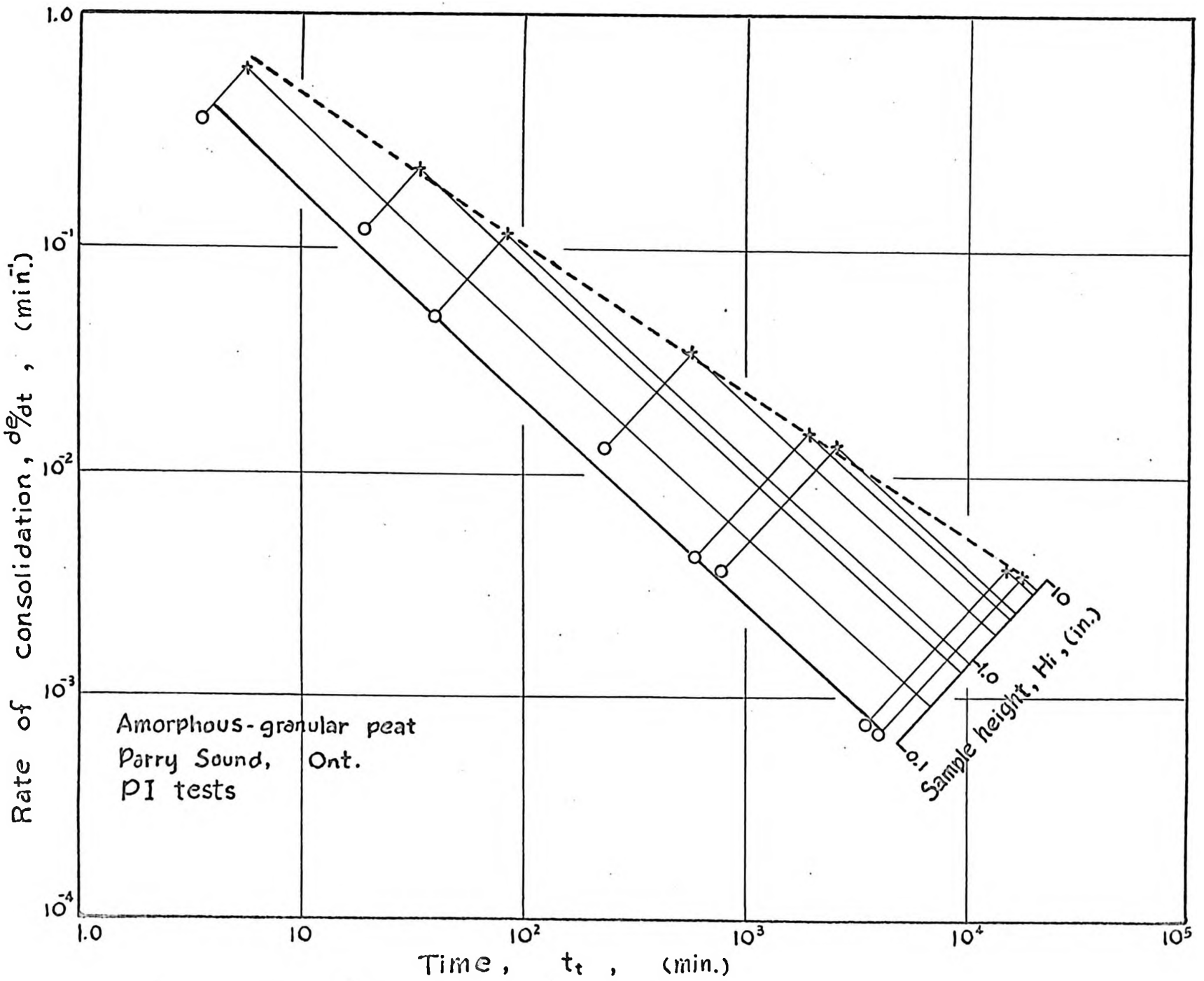

Fig. 14. $d\varepsilon/dt - t_t - Hi$ at the "End of early stage" consolidation.

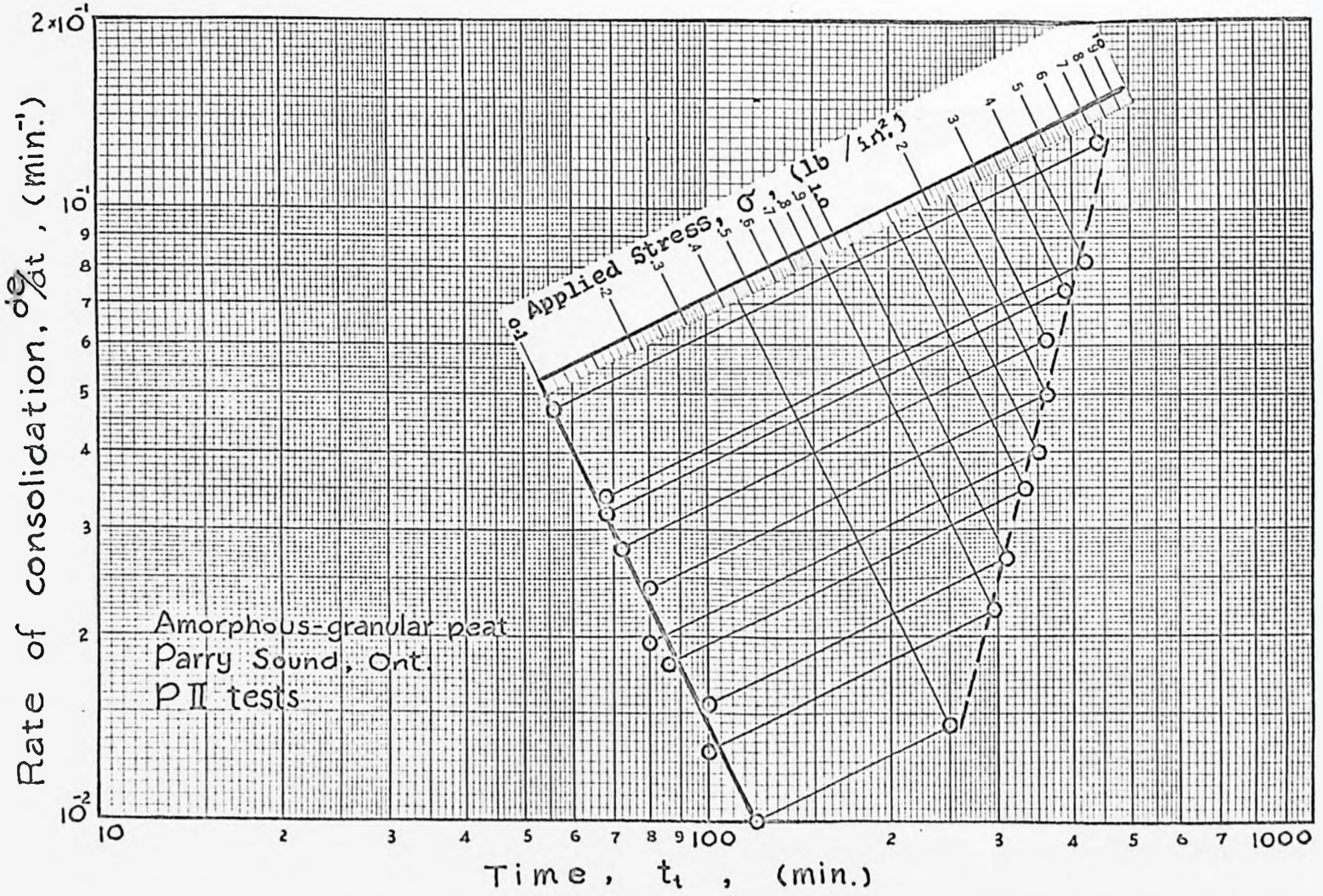

Fig. 15. $de/dt - t_t - \sigma$ at the "End of early stage" consolidation.

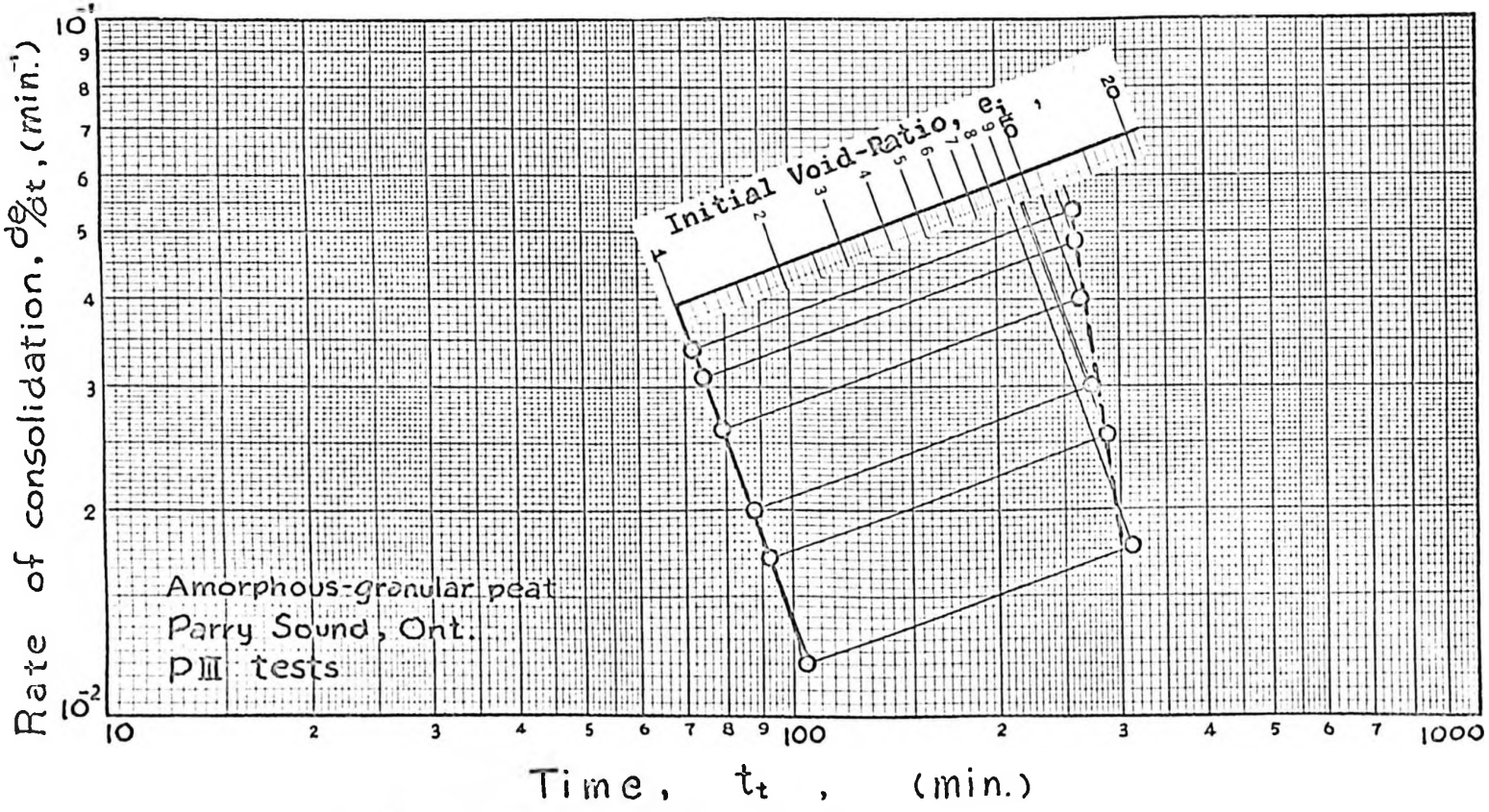

Fig. 16. $d_e/d_t - t_t - e_i$ at the "End of early stage" consolidation.

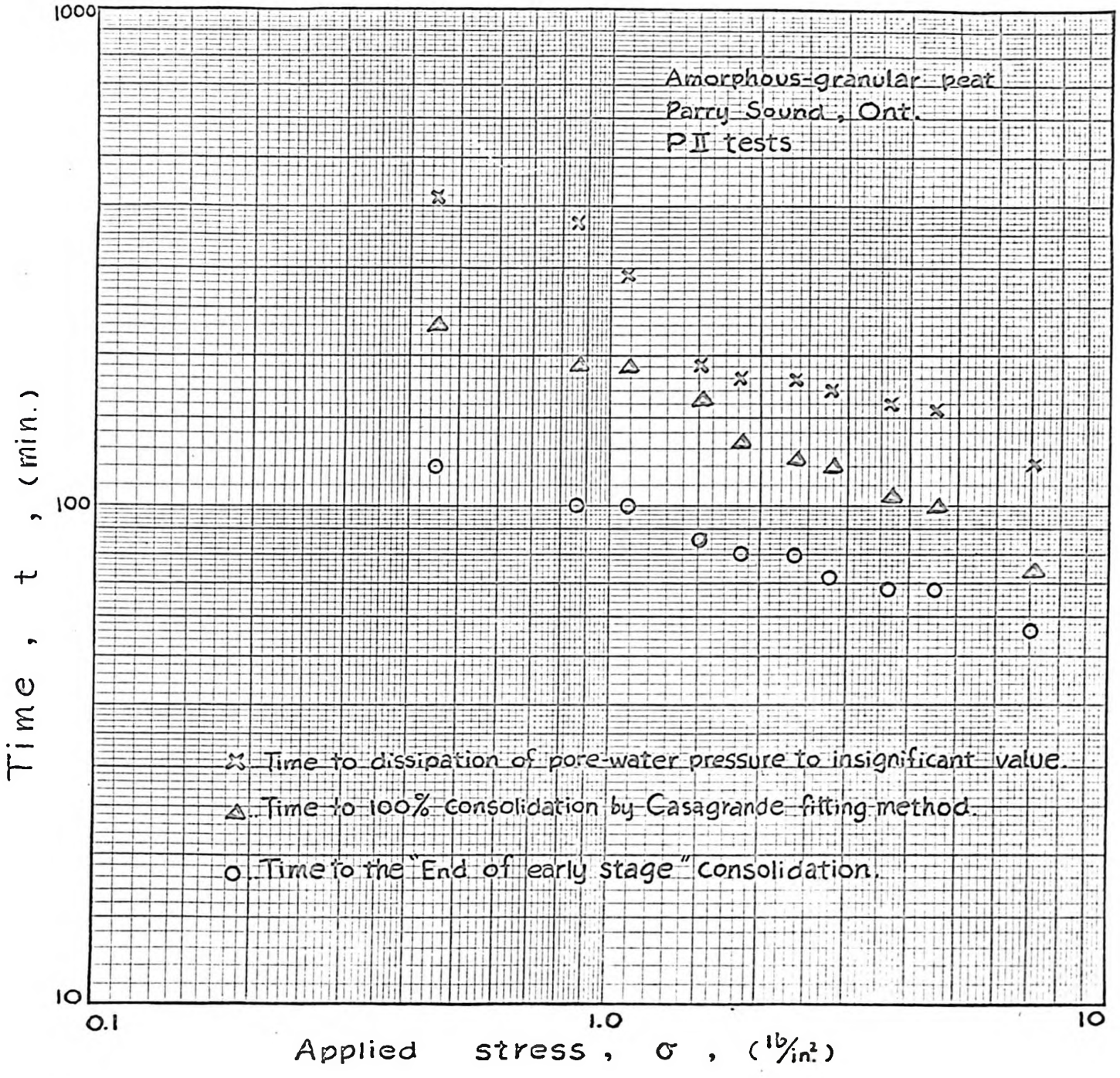

Fig.17. Comparison of fitting methods.

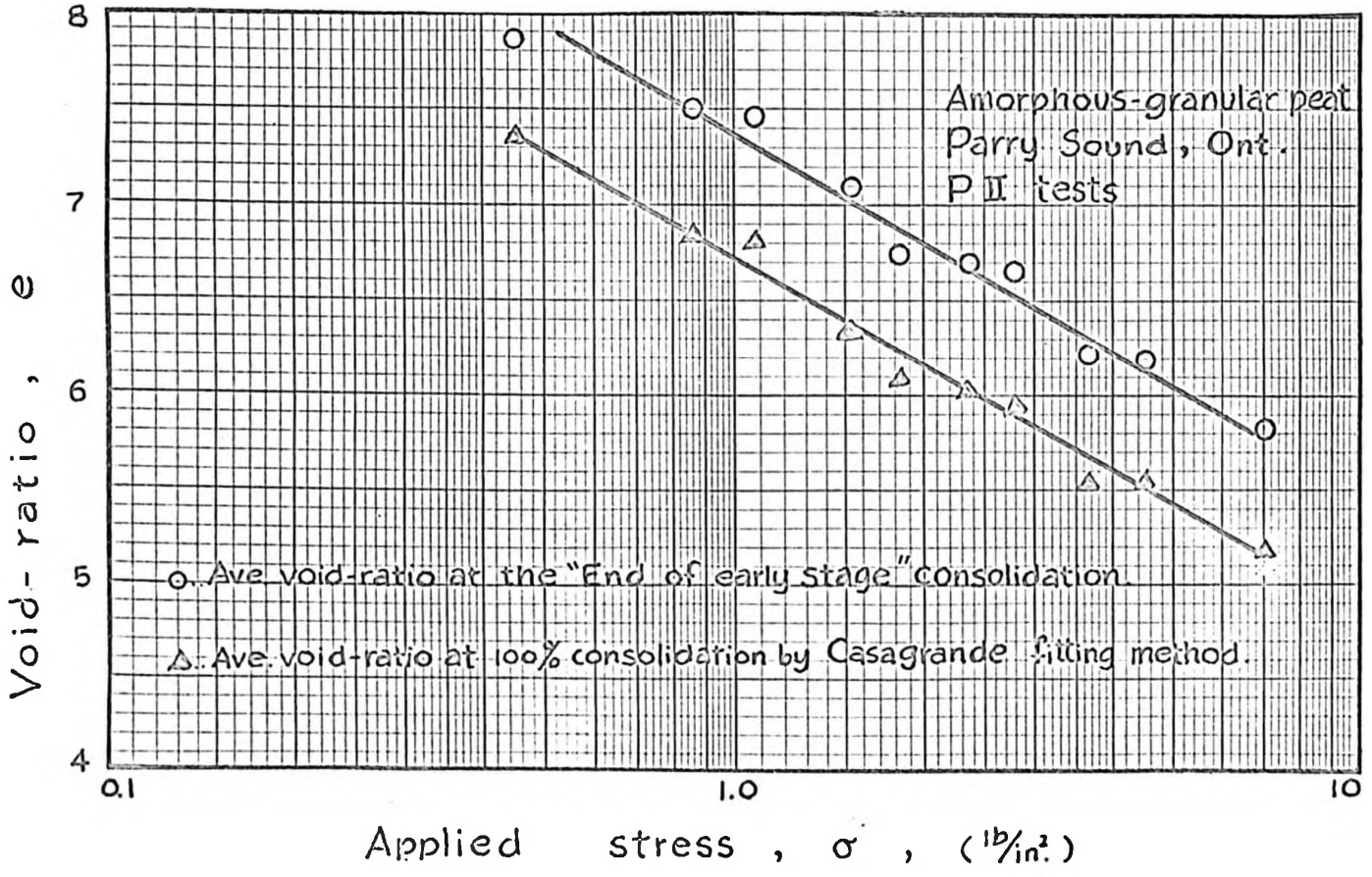

Fig. 18. Comparison of e - log σ curves.

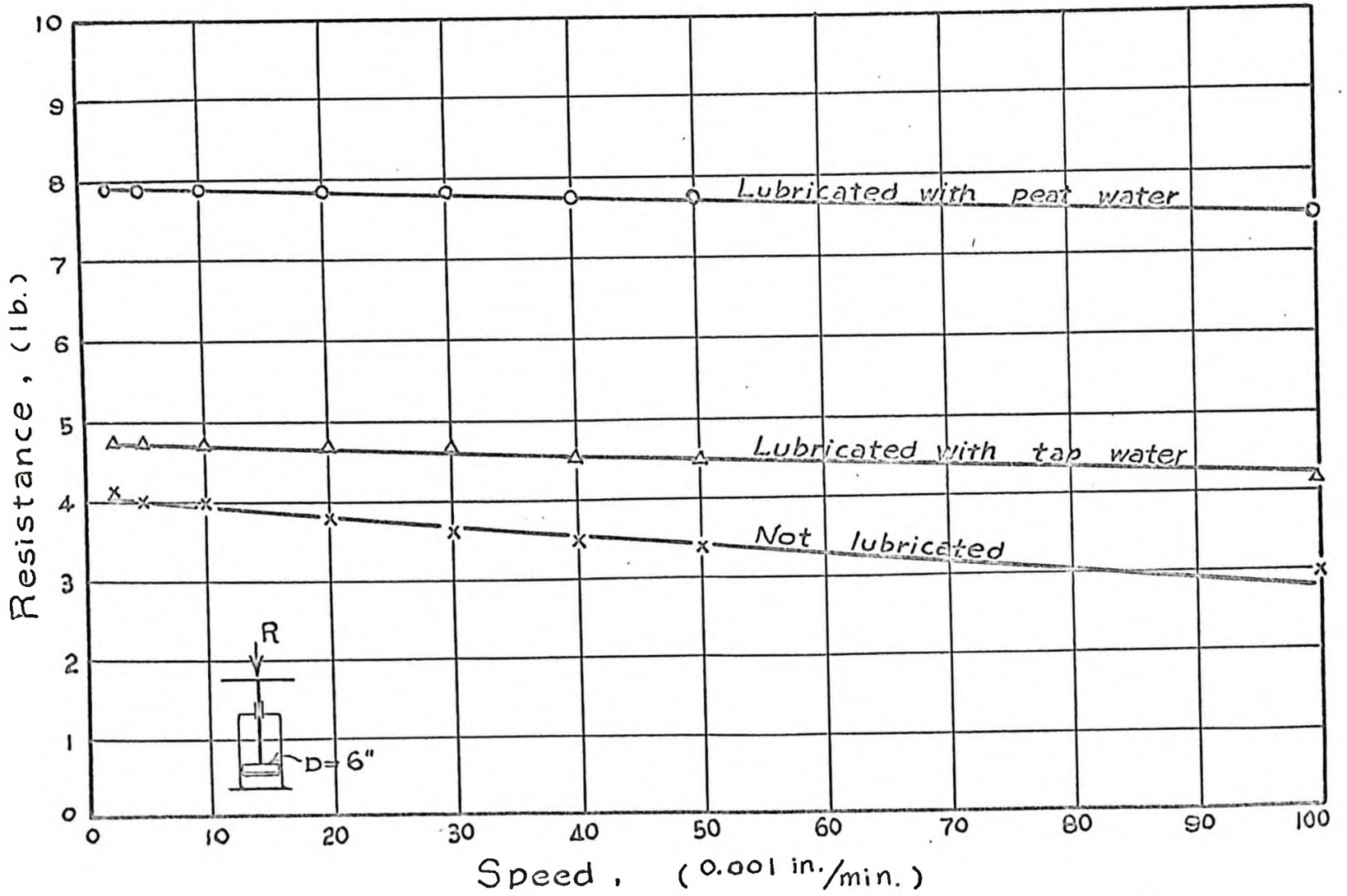

Fig. 19. Calibration chart for piston resistance.